

Vehicular Channel Characterization and Its Implications for Wireless System Design and Performance

By CHRISTOPH F. MECKLENBRÄUKER, *Senior Member IEEE*, ANDREAS F. MOLISCH, *Fellow IEEE*, JOHAN KAREDAL, *Member IEEE*, FREDRIK TUFVSSON, *Senior Member IEEE*, ALEXANDER PAIER, *Student Member IEEE*, LAURA BERNADÓ, *Student Member IEEE*, THOMAS ZEMEN, *Senior Member IEEE*, OLIVER KLEMP, *Member IEEE*, AND NICOLAI CZINK, *Member IEEE*

ABSTRACT | To make transportation safer, more efficient, and less harmful to the environment, traffic telematics services are currently being intensely investigated and developed. Such services require dependable wireless vehicle-to-infrastructure and vehicle-to-vehicle communications providing robust connectivity at moderate data rates. The development of such dependable vehicular communication systems and standards

requires accurate models of the propagation channel in all relevant environments and scenarios. Key characteristics of vehicular channels are shadowing by other vehicles, high Doppler shifts, and inherent nonstationarity. All have major impact on the data packet transmission reliability and latency. This paper provides an overview of the existing vehicular channel measurements in a variety of important environments, and the observed channel characteristics (such as delay spreads and Doppler spreads) therein. We briefly discuss the available vehicular channel models and their respective merits and deficiencies. Finally, we discuss the implications for wireless system design with a strong focus on IEEE 802.11p. On the road towards a dependable vehicular network, room for improvements in coverage, reliability, scalability, and delay are highlighted, calling for evolutionary improvements in the IEEE 802.11p standard. Multiple antennas at the onboard units and roadside units are recommended to exploit spatial diversity for increased diversity and reliability. Evolutionary improvements in the physical (PHY) and medium access control (MAC) layers are required to yield dependable systems. Extensive references are provided.

KEYWORDS | IEEE 802.11p; intelligent transport systems; multiple-input-multiple-output (MIMO); orthogonal frequency division multiplexing (OFDM); radio channel characterization; vehicular communications

Manuscript received June 23, 2010; revised October 7, 2010; accepted December 1, 2010. This work was supported in part by the Swedish Strategic Research Foundation (SSF) under INGVAR Grant, the SSF Center of Excellence for High-Speed Wireless Communications (HSWC), the FTW projects REALSAFE and ROADS SAFE, Christian Doppler Lab for Wireless Technologies for Sustainable Mobility, COST2100, and NewCom++. The work of T. Zemen was supported by the Vienna Science and Technology Fund (WWTF) through the FTW Project COCOMINT. The FTW Telecommunications Research Center Vienna is supported by the Austrian Government and the City of Vienna within the competence center program COMET.

C. F. Mecklenbräuker and **A. Paier** are with the Institute of Telecommunications, Vienna University of Technology, Vienna A-1040, Austria (e-mail: cfm@nt.tuwien.ac.at; apaier@nt.tuwien.ac.at).

A. F. Molisch is with the University of Southern California, Los Angeles, CA 90037 USA (e-mail: molisch@usc.edu).

J. Karedal and **F. Tufvesson** are with the Department of Electrical and Information Technology, Lund University, Lund 221 00, Sweden (e-mail: Johan.Karedal@eit.lth.se; fredrik.tufvesson@eit.lth.se).

L. Bernadó, **T. Zemen**, and **N. Czink** are with the FTW Telecommunications Research Center Vienna, Vienna A-1220, Austria (e-mail: bernado@ftw.at; thomas.zemen@ftw.at; czink@ftw.at).

O. Klemm is with BMW Group Research and Technology, 80937 Munich, Germany (e-mail: oliver-klemm@t-online.de).

Digital Object Identifier: 10.1109/JPROC.2010.2101990

I. INTRODUCTION

Research into vehicular channels gained strong momentum during 2006, when the Wireless Access for Vehicular Environments (WAVE) initiative and other vehicular applications spurred interest in *dependable* vehicular connectivity. Dependable connectivity is crucial for intelligent transport systems (ITSs), i.e., reliable low-latency vehicular communication links that are capable of meeting strict packet delay deadlines.

ITSs require both vehicle-to-infrastructure (V2I) and vehicle-to-vehicle (V2V) communications. It is envisioned that all road users gather sensor data about traffic and road state information, and exchange these data among each other and with the road infrastructure. Each vehicle can thereby aggregate and share information for safety improvements [1], e.g., collision avoidance, emergency vehicle warning, hazardous location notification, wrong-way driving warning, cooperative merging assistance, traffic condition warning, slow vehicle warning, and lane change assistance. Such applications will prevent traffic accidents by periodically monitoring the locations of surrounding vehicles aided by event-triggered messages.

Since the quality of the local map depends on the behavior of each individual communication link, vehicle dynamics and propagation conditions ultimately define the reliability and robustness of vehicular communication systems. The challenging properties of the wireless communication channel have a strong impact on the communication system design and the obtainable performance in ITSs. Vehicular channels generally are *randomly time varying* [2]: their identifiability from measurements, statistical characterization, and modeling is rather challenging [3]–[7].

An international standard, IEEE 802.11p [8], which is part of the WAVE initiative, has gained considerable importance. Based on the popular WiFi standard, it is intended for both V2I and V2V traffic telematics applications, and operates in the 5.9-GHz band. Its importance is further highlighted by the European decision on the use of the 5875–5905-MHz frequency band for safety-related ITS applications [9]. Further extensions to the standard are currently under development [10]–[12]. We note that a 700-MHz band is devoted to advanced driving safety support systems in Japan [13]. IEEE 802.11p is also one mode of communication access for land mobiles (CALM), a framework for heterogeneous packet-switched communication in mobile environments approved by the International Standards Organization (ISO).¹ Summarizing, the IEEE 802.11p standard has established itself as the key technology for V2V and V2I communications.

¹The CALM framework supports user-transparent continuous communications across various interfaces and communication media, including CALM M5 (based on IEEE 802.11p), 2G/3G/4G cellular systems, and more.

Since 2006, a large number of papers have been published in this field by a growing number of research groups all over the world [14]–[20]. The goal of this paper is twofold: 1) help communications system designers to gain an overview of the vehicular channel characteristics; and 2) let propagation researchers assess where the most pressing needs for further work lie.

The paper is organized as follows. In Section II, we discuss vehicular propagation channels, including application-specific scenarios, the impact of vehicle types, and antennas. Section III assesses the associated needs for wireless system design. Finally, we formulate open issues and suggestions for future research and development.

II. VEHICULAR PROPAGATION CHANNELS

A. Channel Properties

In a wireless link, the signal propagates from the Tx (transmitter) to the Rx (receiver) via several propagation paths. The contributions of those paths add up at the Rx. As a result we experience fading, variation of the received signal power with time, and signal echoes with different delays. The contributions of the various propagation paths, i.e., amplitudes and phases, and their respective delays define the *impulse response*. The expected (i.e., averaged) power at different delays is described by the average power delay profile (APDP), from which the so-called root mean square (rms) delay spread is evaluated as the second central moment [21].

For vehicular channels, it is customary to distinguish between V2V and V2I channels. These channels not only differ from each other, but also deviate significantly from those in cellular communication. In cellular scenarios, the base station (BS) is fixed, elevated, and located at or above rooftop level, such that its close surroundings are free of scatterers. Furthermore, most of the relevant scatterers are immobile or move fairly slowly. The distance between the BS and the user spans roughly from 10 m to 10 km.

In a V2V communication scenario there is neither access point (AP) nor BS and both the Rx and the Tx may move with high velocities. The antennas are mounted at a height of 1–2 m, many relevant scatterers (i.e., vehicles) move, and the distances between the Tx, the Rx, and important scatterers are in the range of a few hundred meters. Depending on whether the scenario includes a road in an open field or a busy street in an urban environment, the number of relevant scatterers might vary significantly.

In a V2I scenario, the propagation channel is similar to a cellular microcell scenario if the BS/AP antenna is elevated. However, if the BS antenna is at low height, the channel becomes similar to a V2V scenario with the important difference that the expected velocities of scatterers and the mobile node need not be identical in both cases.

All these properties influence the input–output relationship of the channel, i.e., how signals propagate from the transmitters to the intended, and other nonintended, receivers. Since these relationships vary between different scenarios, it is highly unlikely that a wireless system optimized for one specific scenario will also work well in other, completely different, scenarios.

Channel Metrics: The following five properties mainly characterize wireless channels. 1) *Pathloss:* How does the average received power level vary with distance to the transmitter? 2) *Signal fading:* How does the instantaneous signal level fluctuate over time, frequency, and space? 3) *Delay spread:* How is the signal smeared in time by echoes? 4) *Doppler spread:* How is the transmitted signal smeared in frequency due to movements of the Rx, the Tx, and scatterers? 5) *Angular spread:* How is the transmitted signal smeared over directions by antennas and scatterers?

The pathloss and fading strongly influence the performance since they determine the instantaneous signal-to-noise-and-interference ratio. We distinguish between distance-dependent pathloss, large-scale fading, and small-scale fading. For a given frequency, the received power level in decibel is modeled as

$$P(d) = P_0 - 10n \log_{10}(d/d_0) + X_\sigma + Y \quad (1)$$

where d is the distance, P_0 is the power level at the reference distance d_0 , n is the pathloss exponent, and X_σ and Y are the large- and small-scale fading contributions, respectively. Fig. 1 exemplifies the instantaneous power level variations when two vehicles are approaching each other in a highway scenario.

The large-scale fading is modeled as a log-normal variate, meaning that X_σ has a Gaussian distribution with

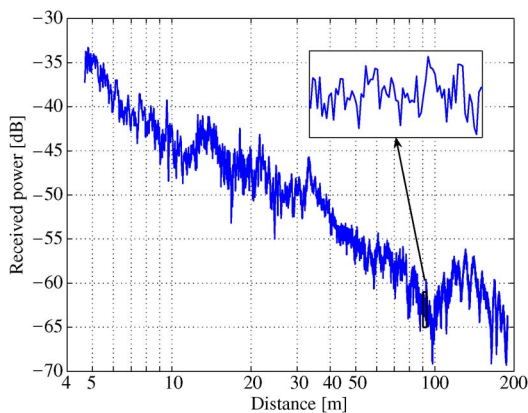


Fig. 1. Example of variations of the received power level in a highway scenario when two vehicles are driving in opposite directions. The inset figure shows the small-scale variations.

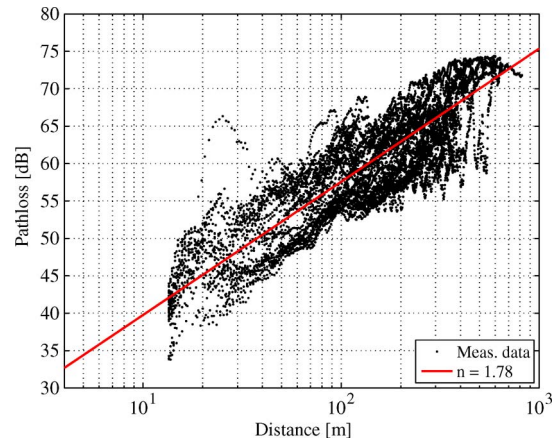


Fig. 2. Scatter plot of the small-scale averaged power loss compared to the distance-dependent pathloss (from [23]).

standard deviation σ , whereas Y is modeled as a Rician [22], Rayleigh, Nakagami, or Weibull [14] distributed variate. We emphasize that both small- and large-scale fading variates are correlated in time, however at different time scales. The coherence time of the small-scale fading is determined by the Doppler spread and depends on the movements of vehicles and scatterers whereas the correlation distance of the large-scale fading is determined by the environment, other cars, and the road’s surroundings. Fig. 2 shows a scatter plot of the instantaneous pathloss compared to the distance-dependent pathloss measured in a highway scenario. Note the deviations (of up to ± 10 dB in this case) from the distance-dependent pathloss. The delay spread is a measure of the memory of the channel and determines the coherence bandwidth of the channel, i.e., the frequency separation over which one may assume the channel to have roughly the same transfer function. The coherence bandwidth B_{coh} is estimated as

$$B_{\text{coh}} \approx \frac{1}{2\pi\tau_{\text{rms}}} \quad (2)$$

where τ_{rms} is the rms delay spread of the channel. The delay spread may change considerably from environment to environment and also over time while driving within one and the same environment.

The Doppler spread quantifies how fast the channel changes and how much a pure sinusoidal carrier is smeared over a frequency band. The coherence time of the channel can be estimated as

$$T_{\text{coh}} \approx \frac{1}{2\pi f_D} \quad (3)$$

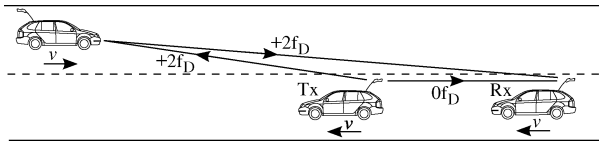


Fig. 3. Doppler shift for two vehicles when driving in the same direction and with a mobile scatterer driving in the opposite direction.

where f_D is the Doppler spread. The maximum Doppler frequency in a V2V scenario can be up to four times higher than one would encounter in a cellular scenario with the same velocity. This is due to the movements of the Tx, the Rx as well as the relevant scatterers in the V2V scenario. Consider, e.g., two vehicles (one Tx and one Rx vehicle) driving in the same direction with a mobile scatterer (another vehicle) driving in the opposite direction (see Fig. 3).

All vehicles have the same speed. If the Tx is approaching the mobile scatterer this contributes to the Doppler shift by a value corresponding to twice the speed of the single vehicle. Since now also the Rx is approaching the mobile scatterer, there is a second contribution to the Doppler shift corresponding to twice the speed of a single vehicle. In total the Doppler shift corresponds to four times the speed of the single vehicle. Further, we emphasize that the short-term Doppler spectrum may change rapidly in a vehicular channel, which implies that the conditions for wide-sense stationarity are violated [24].

Finally, the angular spread is a key quantity for the design and evaluation of vehicular antennas. As described above, different echoes of the transmit signal, so-called multipath components (MPCs), are superimposed at the receiver, giving rise to fading. For a complete description of the channel we should use a double directional channel description that additionally assigns an outgoing angle at the Tx and an incoming angle at the Rx to each MPC. Using the double-directional channel description, the design and analysis of directive antennas is possible. Directive antennas suppress MPCs from specified directions whereas a higher sensitivity is provided elsewhere. For multiantenna systems, such directivity can be achieved by electronic beamsteering. From a system perspective the angular spread determines the spatial coherence of the channel, which becomes a key channel property when designing multiantenna arrays. It further determines the potential power gains: A low angular spread indicates a large potential for power gain by beamforming. Conversely, a large angular spread indicates a large potential for diversity gain.

B. Propagation Environments and Application-Specific Scenarios

The characteristics of vehicular propagation channels depend on the nature of the surrounding environment. For this reason, vehicular measurement campaigns have been

carried out in various propagation environments; see, e.g., [14]–[19]. The campaigns are conducted by letting two vehicles drive in convoy or in opposite directions while measuring (V2V), or by parking one of the vehicles to emulate V2I (more information about V2I can be gleaned from cellular measurements; see Section II-D). The most common environments, *urban*, *suburban*, *highway*, and *rural*, have also been widely investigated for cellular systems.

- *Urban* streets are often wide, with one or two lanes in each direction, though regional differences apply. The streets in the United States are usually wider and straight, whereas European city streets can be narrow and winding. In this environment, houses are close to the curb and the traffic density is typically high.
- In *suburban* areas, there are usually one or two lanes in each direction. In contrast to urban streets, the suburban streets are narrower, and the houses are more set back from the curb. Again, there may be large variations depending on culture and country; in the United States the houses are often set back 8–10 m from the curb, whereas this distance is much smaller in Europe and Japan. A light traffic density is typical in suburban areas.
- *Highways* usually have two to six lanes in each direction and lack houses in their immediate vicinity. There is often a divider separating the two directions of travel, and many highways, especially in Europe, are constructed with structures for reducing traffic noise (e.g., earth berms or sound abatement walls). The traffic density ranges from very high on urban highways (up to 10 000 vehicles/h), to considerably lower levels on highways through rural areas (e.g., many interstate highways in the United States).
- *Rural* roads typically have a single lane in each direction and few or no buildings next to them, though hills and vegetation can provide additional multipath components. The traffic density is usually light.

For many of the applications for which vehicular networks are envisioned, e.g., approaching emergency vehicle warnings, hazardous location notifications, or traffic condition warnings, the classification by propagation environment is reasonable, as these applications will be useful for practically any type of roads. There are, however, also various *application-specific scenarios* for which this classification is insufficient and where there is a need for dedicated channel characterization [25]. Such applications include both precrash and postcrash warnings. Two examples for precrash warnings are intersection collision avoidance and cooperative merging assistance. Postcrash warnings are intended to facilitate traffic flow after the occurrence of a traffic accident by broadcasting a message with the accident's location so that approaching vehicles can circumvent the accident.

As an example, consider intersection collision avoidance, where radio communication is intended to help the drivers become aware of hazardous vehicles with which they lack visual contact. This is expected to be useful when another vehicle is in danger of running a stop sign or traffic signal, and at a left turn. Even though intersections exist in all of the aforementioned environments, it is first and foremost the “intersection-specific” characteristics that need to be properly assessed, e.g., how the line-of-sight (LOS) path is obstructed by building structures when two cars approach an urban intersection from perpendicular directions. Since convoy and opposite direction measurements often miss these effects, those results are not applicable for characterizing channels in intersections.

In intersection collision avoidance systems, either V2I or V2V communications may be used. In the latter case, the LOS path of the propagation channel between vehicles that are in risk may well be obstructed while approaching the intersection. Thus, the success of the transmitted warning message depends on the availability of other significant propagation paths via surrounding buildings and other vehicles. This was investigated in [26], where vehicle-to-vehicle propagation channels for four different types of intersections, differing in terms of size (width, number of lanes, etc.), availability of LOS, adjacent buildings, and traffic density, were investigated.

Other specific scenarios for collision avoidance applications include blind lane merges and slow traffic warnings. The latter is of interest for a vehicle approaching a highway congestion. The congestion scenario is also relevant for postcrash applications, since emergency vehicles and other vehicles arriving at the crash site will quickly turn it into a congestion-like situation. The large vehicle density in congestion gives rise to radio propagation channels with an obstructed LOS path, but may also provide a large number of significant propagation paths. Obviously, the antenna placement has a major influence on the significance of these effects [27], e.g., a roof-mounted position is less likely to suffer from LOS obstruction. Tunnels are another example of a postcrash application-specific scenario. For safety reasons, it is highly desirable to avoid having a large number of vehicles stuck inside a tunnel in which a collision has occurred.

C. Vehicular Antennas

Due to the multipath propagation discussed in Section II-A, antenna-related effects affected by the vehicular mounting position and mutual coupling play an integral role in the performance of vehicular communications (especially V2V).

V2V communications is predominantly taking place in the horizontal xy -plane thus requiring terrestrial coverage of the V2V antenna frontend. Due to the plethora of different use cases for ITS (e.g., highway versus traffic intersection) as well as the relative movement and direction of vehicles in the horizontal plane, an omnidirectional cover-

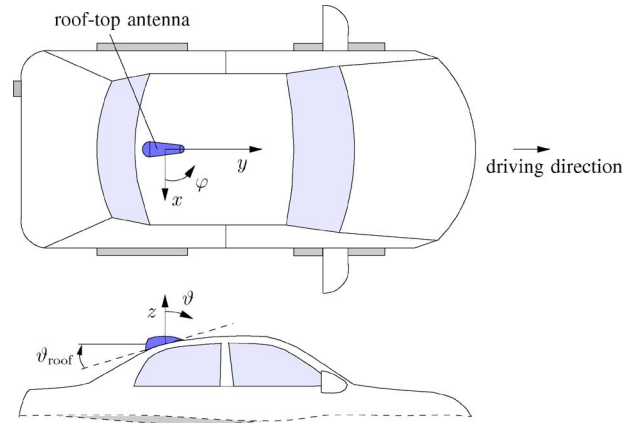


Fig. 4. Antenna mounting and coordinates for antenna radiation pattern.

age of the V2V antenna beam pattern for all azimuth angles φ with maximum gain at elevation $\vartheta = 90^\circ$ (i.e., in the horizontal plane) is highly desired. Fig. 4 depicts the coordinate definition of the antenna radiation pattern relative to the vehicle. Omnidirectional coverage in azimuth ensures reasonable transmission properties for all possible combinations of angles of departure at the Tx and angles of incidence at Rx. In V2I communications, the beam pattern layout for the vehicular antenna is usually less restrictive since link quality and its associated fading statistics generally exhibit improved conditions in comparison to V2V communication links. From a design and cost perspective, V2I and V2V communications need to share the same antenna installation: since the difference in the elevation angle between vehicular- and infrastructure-mount antennas is comparatively small, one vehicular antenna installation can serve the requirements for both V2I and V2V communications.

Even though the antenna design methodology for V2V antennas is already well explored,² predominantly the conventional automotive mounting concepts affect the overall system performance metrics and significantly contribute to its limits [28], [29]. It is shown in [30] that proper antenna placement on the vehicle shell ultimately defines the quality of the radio link and limits its performance metrics.

The desired omnidirectional antenna coverage in azimuth conflicts with the conventional mounting positions on vehicles as depicted in Fig. 4. A relevant position for automotive-compliant V2V antenna equipage is given by the conventional rooftop antenna module. This one is centered and located at the back of the metallic vehicle roof. The vehicle roof itself provides some properties that

²Since a terrestrial beam coverage is required, mostly derivatives of monopole-like antenna prototypes can be used on top of the metallic enclosure of the vehicle to illuminate the xy -plane.

negatively influence the radiation pattern of V2V antennas: It represents a metallic surface with finite dimensions with, e.g., potential insets for nonmetallized sun roofs or railings oriented in parallel to driving direction. In addition to the railings that cause shadowing to the left and right sides of the vehicle, the roof provides a finite inclination ϑ_{roof} at the mounting position of the rooftop antenna. This angle depends on the vehicle type and can be in the range of $\vartheta_{\text{roof}} \in [10, \dots, 15]^\circ$ for sedan cars. As a result of the inclination, the overall embossing of the vehicle roof may therefore cause significant shadowing in driving direction. Therefore, the performance metrics of vehicular-mounted antennas in V2V communications depends on the type of the vehicle: Sedan and convertible cars impose even more challenging requirements to the antenna design in comparison to truck or minivan vehicles with an almost flat roof. Conventionally, the rooftop antenna module provides functionality for several broadcasting and telecommunications services. Those typically include antennas for cellular communications and global positioning system (GPS) as well as for satellite radio services [e.g., US satellite digital audio radio systems (SDARSs)]. Generally, the entire rooftop antenna equipment is enclosed by a dielectric housing that protects against environmental influences and which is subject to aesthetic design considerations. We summarize the effects affecting the performance for rooftop mounted V2V antennas:

- beam tilt in elevation ϑ due to limited vehicle rooftop;
- shadowing of radiation pattern due to inclination ϑ_{roof} ;
- mutual coupling of antenna elements enclosed within the rooftop antenna module;
- coupling with the dielectric housing of the antenna module.

In addition, multiple antenna techniques have gained considerable attention in the field of vehicular communication systems as shown in Section III. In this context, we need to distinguish between *measuring the channel* with multiple antenna elements and *implementing multiple antenna technology* for vehicular communications. Measuring with multiple antenna elements is beneficial, since it allows directional resolution of the channel, which in turn gives new insights into propagation effects, and allows to analyze the impact of the radiation pattern of (single-element) antennas, as well as being vital for performance analysis of multiantenna operation. In compliance with the current WAVE standard, multiple antenna elements can be applied for Tx and Rx beamforming, as well as Rx diversity. Generally, multiple antenna techniques enable improved system reliability and robustness in vehicular communications. Multiple antennas allow to compensate for some of the integrational impairments that occur during series production. Their application can enhance network scalability and interference management in heavily loaded V2V networks. Exploiting spatio-temporal fading phenomena,

multiple antenna techniques increase implementation margins in typical multipath propagation scenarios such as in Fig. 8. Those additional performance gains may prove to be a significant precondition for a reliable operation of V2V communication equipment for safety applications. The question whether to deploy multiple antennas in vehicular onboard equipment strongly depends on the outcome of various field operational tests [31], [32] deriving relevant performance metrics in safety-relevant use cases. However, the available degrees of freedom for placement of multiple element antennas are rather limited: Due to aesthetic design and cost considerations, the automotive industry strongly restricts the number of mounting positions for antenna equipment on the vehicle shell and their locations. Architectural constraints especially limit the potential to apply multiple antennas for 5.9-GHz antennas for ITS services in series productions: Conventionally, the bus architecture foresees signal processing in a centralized control device located in the vehicle's head unit. This architecture includes radio-frequency (RF) to baseband conversion in the head unit leading to a significant deterioration in signal-to-noise ratio (SNR) due to cable assembly. Connection lengths up to 8 m in large series vehicles call for low-loss cable assembly as a precondition for meeting sensitivity limits at the receiver. Since multiple antennas require multiple connection lines from the antenna housing to the control unit, such an architecture is at an disadvantage concerning the bill of materials. Alternative antenna locations, e.g., integration into the side mirrors, require even more sophisticated cable assembly including flexible connection lines and rotary joints which further increase the bill of materials. The drawbacks of this electrical bus architecture are resolved by displacing relevant functional units comprising RF to baseband conversion and signal processing from the head unit to the rooftop antenna location. This architectural concept of a centralized RF gateway close to the antenna module would enable the operation of multiple antennas for ITS at 5.9 GHz. As displayed in Fig. 5, a digital bus interface connects the RF gateway with the head unit.

As an example, the aforementioned mounting positions are considered for a V2V antenna design based on a short-circuited circular patch, excited in its fundamental mode [33]. Antenna elements of this kind feature a monopole-like radiation pattern for near-omnidirectional, terrestrial

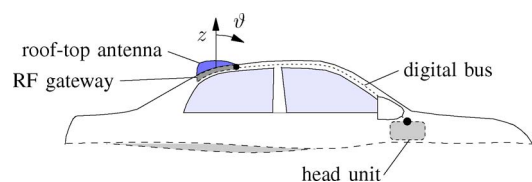


Fig. 5. Electrical vehicle architecture including centralized RF gateway to enable multiple antenna operation.

coverage. They provide some limited headroom for beam shaping in elevation ϑ . Fig. 6 highlights the effects of the vehicular antenna integration on a metallic rooftop with finite dimensions at 5.9 GHz. Fig. 6(a) represents the vertical antenna gain of the short-circuited patch antenna, which is centered on the rear part of the vehicle rooftop. A major consequence of the mutual coupling with the induced currents on the rooftop is a shift of the main beam from $\vartheta = 90^\circ$ to an angular range at $\vartheta \simeq 72^\circ$. The beam tilt ultimately causes a degradation of the SNR for vehicular transmitters located in the horizontal plane. The mean gain reduction in the horizontal plane caused by the finite size of the vehicle roof is around 4 dB.

The severity of this mounting-based degradation of the V2V antenna performance in the horizontal plane becomes more pronounced in case of a realistic tapering of the vehicle roof with a bent angle of $\vartheta_{\text{roof}} = 10^\circ$ as depicted in Fig. 6(b). As a consequence, sedan- and sport utility vehicle (SUV)-type cars featuring different roof tapering conditions also differ in their beam pattern performance. These differences in mounting result in a drop of directive antenna gain to approximately -6.5 dB in driving direction ($\vartheta = 90^\circ$ and $\varphi = 90^\circ$ with coordinates defined according to Fig. 4), thus yielding a significant sensitivity loss of the associated receiver hardware.

The current trend in automotive manufacturing considers the integration of large glass insets in the vehicle roof especially for mid- and high-price vehicles. Due to the modified electromagnetic boundary conditions, this trend will affect the coupling with the metallo-dielectric surroundings of the vehicle shell. It may even call for alternative antenna design rules including symmetrically fed antenna designs.

The effect of the dielectric antenna housing can be seen in Fig. 7. Calibrated radiation pattern measurements of the short-circuited patch antenna were taken at 5.6 GHz in a spherical near-field chamber. This operating frequency was used in the measurement campaign. It is very close to

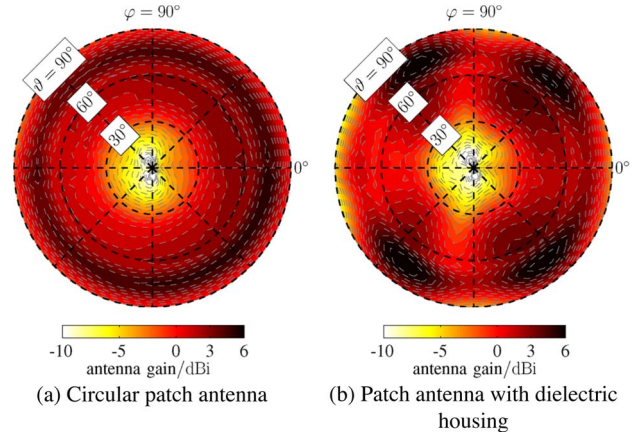


Fig. 7. Measurement of antenna radiation pattern with custom design cover: (a) antenna without cover and (b) antenna with cover.

the allocated 5.9-GHz frequency band for ITSs in Europe such that a different behavior of the radio channel is not expected. Fig. 7(a) shows the results of the standalone antenna mounted at the center of the ground plane, whereas Fig. 7(b) represents the radiation pattern including an automotive-compliant, dielectric design cover. We observe that the dielectric housing of the rooftop module leads to a significant deterioration of the related antenna radiation patterns. Due to the limited size of the rooftop module that are typically in the order of (60×110) mm, Fig. 7(b) shows the geometry- and frequency-dependent interference pattern resulting from reflection and refraction effects inside the antenna housing. Due to the symmetric arrangement, the electromagnetic interactions within the antenna housing yield an azimuthal modulation of the associated far-field patterns with a periodicity of 180° in azimuth φ . The resulting peak-to-peak variation amounts to approximately 5 dB in the horizontal plane ($\vartheta = 90^\circ$). As shown in [34], mutual coupling with additional antennas enclosed in the same rooftop compartment causes beam steering of the V2V antenna module hence altering its omnidirectional coverage. This may lead to further impairments of the link.

Besides the traditional mounting position on the vehicle roof, vehicle manufacturers explore alternative mounting sites for V2V antenna equipment, as surveyed in, e.g., [30]. Such alternative mounting sites are the front and rear bumpers, the left and rear side mirrors as well as the bottom of the vehicle itself. Resulting performance of multiple-antenna systems is compared in [35] and [36]. It must be noted that choices for alternative mounting concepts are driven not only by performance, but also by cost and aesthetic design considerations.

Finally, we note that the smaller size of the underlying resonant antenna structures (compared to cellular antennas) calls for stringent manufacturing requirements during batch production and *in situ* vehicular integration. The

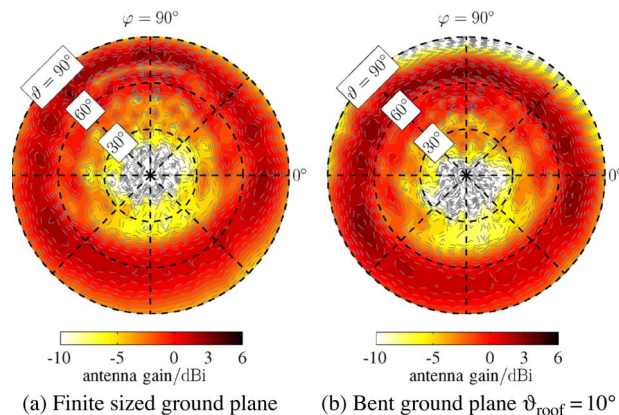


Fig. 6. Antenna radiation patterns on finite sized ground plane with (a) $\vartheta_{\text{roof}} = 0^\circ$ and (b) $\vartheta_{\text{roof}} = 10^\circ$ of elevation.

latter is due to the fact that, e.g., mechanical tolerances from slots or grooves in the vehicle roof might already be in the order of magnitude of the operational wavelength, thus deteriorating the beam pattern performance.

D. Vehicle-to-Infrastructure Channels

When considering V2I communications, we first need to define precisely what we mean by “infrastructure.” We distinguish two cases: 1) conventional cellular infrastructure, e.g., following the Third Generation Partnership Project (3GPP) or Worldwide Interoperability for Microwave Access (WiMAX) standards, which is to be used for vehicular communications *in addition to* conventional (human-generated) voice/data traffic; and 2) dedicated infrastructure for ITS connectivity following the IEEE 802.11p standard. In either case, the communication occurs between a device in a vehicle and an elevated infrastructure point, which is the traditional setup in cellular communications. This dates back to the days when cell-phones were known as “car phones,” because they were installed in cars, received their operation power from the car battery, and had an *external* antenna on the car. Thus, investigations of the V2I propagation channel can draw on the results of many decades of cellular propagation measurements. In the current section, we review some of the most important results; more extensive reviews are given, e.g., in [21], [37], and [38]. In that context, we distinguish the following scenarios.

- Macrocells cover *rural, suburban, and parts of urban areas* that are not considered as priorities during initial rollout of dedicated WAVE infrastructure.
- Microcells cover *urban/metropolitan areas* either by “conventional” microcellular BSs, or dedicated WAVE infrastructure. The deployment, and propagation characteristics, of these two cases is very similar. BSs/APs are placed typically at lamppost height, predominantly at intersections (so that both streets are covered at once), but in any case will be much lower than the height of the rooftops of surrounding buildings.
- Tunnels are coverable by cellular and WAVE infrastructure whose placements are the same. Covering tunnels is of high interest to ITS for traffic jam/accident avoidance.
- Highways: We anticipate that WAVE APs are placed at car height on highways, replacing or augmenting the current emergency phone booths. From a propagation point of view, this scenario is similar to a V2V communication. Other areas of highways can be covered by special infrastructure located on overpasses, while highway stretches with low traffic density will most likely be covered by conventional rural macrocell infrastructure.

For many of the above scenarios, most notably macrocells and microcells, standardized channel models exist. We particularly mention the COST 259 Directional Channel

Model [39]–[41], the COST 273 multiple-input–multiple-output (MIMO) model [42], [43] and its extensions by COST 2100 [44], the 3GPP spatial channel model [45], and the WINNER channel model [46] that was recently adopted by the International Telecommunications Union. All of these models provide key parameters, as well as recipes for generating random channel realizations that follow the specified distributions.

1) *Rural Macrocells*: In flat rural areas, there are few propagation obstacles, and most of the scattering occurs in close vicinity to the mobile station. The pathloss in such an environment is well described by the COST 231 Okumura–Hata model (see [21, App. 7A]). The pathloss exponent of this model is given by $n = 4.49 - 0.655 \log(h_b)$, where h_b is the height of the BS. For LOS situations, the pathloss exponent is around 2; for example, Kim *et al.* [47] measured $n = 2.2$. Delay spreads are on the order of 100 ns in flat terrain [41], [48]. In hilly/mountainous terrain, the MPCs interacting with mountains have large delays, and may cause a dramatic increase in the delay spread [49], [50]. Since (in flat terrain) the scatterers are concentrated around the mobile station (MS), the BS “sees” them all within a fairly small angular range; angular spreads of 1° – 5° are typical (e.g., [51]); much larger values are observable in hilly/mountainous terrain.

The variance of the shadowing is relatively low: 6 dB is a typical value; cf. [41].³ The correlation distance of the shadowing is 100–500 m. A vehicle that is in a shadowing dip will remain shadowed on average for the time it takes to traverse this distance.

It is noteworthy that the delay spread, the shadowing, and the angular spread are correlated [52], and are usually modeled as log-normally distributed correlated random variables. Correlation coefficients are usually such that if an MS is in a shadowing dip, it has a higher delay spread and a higher angular spread. Such correlation has not just been observed in rural macrocells, but in other environments as well.

Since most significant scatterers tend to be uniformly distributed around the MS, all MPCs are incident on the MS in the horizontal plane, and the power azimuth spectrum at the MS is isotropic in the horizontal plane. This model is named after Clarke [53], and the associated Doppler spectrum is the “classical” Jakes spectrum [54]. This is, of course, an idealization—the presence/absence of cars in the various lanes, trees/hedges, and possibly buildings near the road all influence the actual scatterer distribution. Still, for rural environments, the Jakes spectrum has been successfully used for system simulations for many years.

³This is the variance of shadowing per cluster. In flat terrain, where there is almost always only the cluster around the MS, this is *de facto* equal to the overall (narrowband) shadowing variance. In hilly terrain, the overall shadowing variance has to be computed from the shadowing per cluster, and the relative strength of the occurring clusters.

2) *Urban and Suburban Macrocells*: In urban macrocells, three propagation phenomena are dominant: 1) scattering around the MS, combined with over-the-rooftop propagation between the MS surroundings and the BS; 2) waveguiding in street canyons; and 3) reflection by remote objects [55]. The relative importance of those processes depends on the construction, as well as the height of the BS compared to the rooftop height of the surrounding buildings. In regularly built-up structures, with the BS significantly above the height of the surrounding rooftops, the first-mentioned process dominates. In that case, the pathloss is well described by the COST 231 Walfish-Ikegami model. In the case of LOS, the pathloss exponent is $n = 2.6$. For NLOS, the overall pathloss (expressed in decibels) is the sum of three terms: the free space pathloss, the multiscreen diffraction loss (the diffraction loss that the waves suffer when passing over the buildings, each of which can be approximated as a “screen” that shadows part of the wave front), and the “rooftop-to-street” diffraction loss, which describes the loss from the roof edge closest to the MS, to the MS (or the objects directly surrounding it). The actual value of the pathloss exponent then depends on the parameters of the building structure, such as spacing between buildings, height of the BS above rooftops, etc. Other popular pathloss models are based on the Hata model: for example, the 3GPP spatial channel model (SCM) suggests $n = 3.5$ for suburban, and urban environments [45]. The shadowing standard deviation is around 6–8 dB [41].

In suburban environments, and urban environments where over-the-rooftop propagation dominates, delay spreads between 100 and 1000 ns are most prevalent [48], [56], [57]. Several measurements show clear examples of multiple clusters that lead to much larger delay spreads (those environments are often called “bad urban” [40], [48]): delay spreads up to 18 μ s, with cluster delays of up to 50 μ s have been measured in various European and American cities [58]–[60]. Also for the angular spread at the BS, the per-cluster spread (which is identical to the overall angular spread if only a single cluster is present) is fairly low (5° – 10°), while the total angular spread can reach up to 40° in the presence of multiple clusters [52].

The angular power spectrum (APS) (i.e., the distribution of the power as a function of the angle) at the MS can show considerable deviations from the Clarke model. MPCs that are undergoing “over-the-rooftop” propagation typically show uniform APS, but an elevation spectrum that is distributed between the horizontal and the angle under which the MS “sees” the nearest roof edge [59]. Kalliola *et al.* [61] found that a double-exponential elevation power spectrum gives a good fit to measured data, with a rather high spread in macrocellular environments. On the other hand, MPCs that propagate along street canyons stay in the horizontal plane, but the azimuthal power spectrum is better approximated as Laplacian centered around the street axis [45]. In either case, the

Doppler spectrum differs significantly from the Jakes spectrum.

3) *Microcells*: In microcells, the BS is situated lower than the surrounding rooftops. As a consequence, the propagation over the rooftop is more strongly attenuated: MPCs suffer from high attenuation both near the BS and the MS. Therefore, waveguiding through street canyons becomes relatively more important. Typical pathloss exponents are $n = 2.3 - 2.6$ for LOS situations, and $n = 3.8$ for NLOS [45]; more detailed models can be found, e.g., in [46] and [62]. Reported shadowing standard deviations vary widely; cf. [45], [46], and [63].

Delay spreads range from around 5–100 ns (for LOS situations) to 30–500 ns (for NLOS) [56], [64], [65]. Angular spreads at the BS are typically larger than in macrocells, with 20° being typical [51], [55].

For the angular spectrum at the MS, and the associated Doppler spectrum, considerations are similar to macrocells. MPCs that are guided along the street canyons show a small elevation spread, and the azimuthal angles at the MS are concentrated close to the street axis. Since street-guided MPCs are dominant in microcells, this effect further determines the characteristics of the overall angular spread at the MS.

4) *Tunnels*: An environment of special interest for V2I communications are tunnels. In an empty tunnel, the dominant propagation mechanism is the LOS and the single-bounce rays, which account for up to 90% of the received power [66]. The pathloss exponent ranges from $n = 1$ to 2. Empty tunnels typically show a very small delay spread (on the order of 20 ns), while tunnels with cars exhibit larger values up to 100 ns [67], [68].

5) *Case Study—Base Station Mounted on Overpass*: As an illustrative example, we discuss the propagation channel between an infrastructure located on an overpass and a car driving on a highway underneath. In this measurement campaign [69], we used multibeam antennas, which consisted of four antenna elements that each had an approximately 90° beamwidth, and steered into orthogonal directions (45° , 135° , 225° , and 315° , where 0° is equal to the driving direction). The APDP over the combined antenna pattern is shown in Fig. 8. With “combined antenna pattern” we mean the sum over all 16 APDPs of the individual single antenna links. We observe a strong LOS contribution throughout the whole measurement run. However, the LOS is interrupted for a 0.3-s interval around the time 6 s, when the vehicle drives under the bridge and only the reflected MPCs reach the Rx. Furthermore, we observe in the APDP that a number of MPCs carry significant power: specular components coming from reflecting objects (other vehicles, trucks, traffic signs, etc.), and diffuse components coming from reflections on vegetation and other small objects surrounding the road.

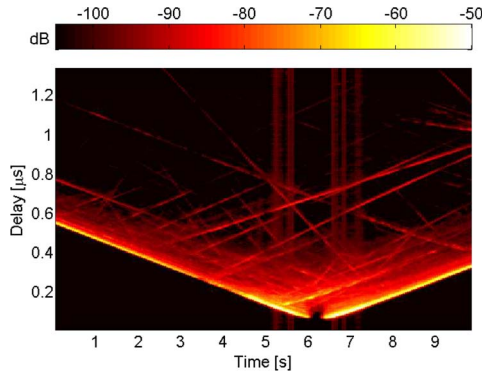


Fig. 8. APDP over the combined antenna pattern for a V2I channel.

The rms delay spread is calculated from the APDP. In the following, we show beside the rms delay spread of the combined patterns also the rms delay spread and channel gain of two single-input–single-output links. The Tx–Rx selected links are denoted as front-to-front and back-to-front. *Front* and *back* indicates the antenna beam direction. In Fig. 9, we show the orientation of the antenna radiation patterns for the Tx and the Rx. When the vehicle approaches the infrastructure, the “front” antenna pattern of the Tx is facing the Rx, and when the Rx vehicle passes by the infrastructure, the “back” antenna pattern of the Tx faces the Rx. We selected these two single links because we consider an infrastructure Tx with beam patterns steered towards the two driving directions of the road (front and back). The beam pattern of the Rx vehicle is considered to face the front, in order to see the different behavior in rms delay spread and channel gain while passing the Tx. The LOS component is diminished at times between 3.1 and 4.4 s. This increases the rms delay spread (depicted in Fig. 10) during that time. Another peak in the rms delay spread is observed when the Rx is under the bridge. The measured rms delay spread values vary from 18.62 to 118.70 ns, with a mean value of 51.99 ns. The channel gain for front-to-front and back-to-front beam pointing is shown in Fig. 11. Intuitively, front-to-front is stronger as the vehicle approaches the bridge, but these two links reverse behavior when the car leaves the bridge. When the

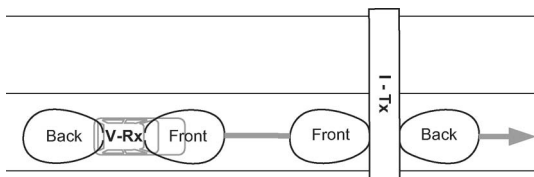


Fig. 9. Antenna beam pattern orientation (“front” and “back”) for the vehicular receiver (V-Rx) and the transmitter at the infrastructure (I-Tx).

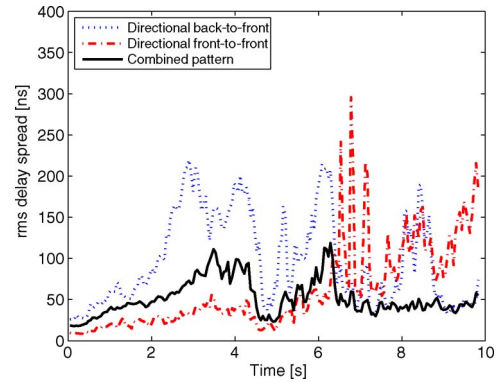


Fig. 10. RMS delay spread for the combined antenna pattern as well as for two single links (back-to-front and front-to-front) for a V2I channel.

Rx remains under the bridge, the channel gain of both links are similar.

E. Vehicle-to-Vehicle Channels

In contrast to V2I channels, V2V channels differ significantly from those of cellular channels, especially in terms of frequency and time selectivity and their associated fading statistics. The investigation of V2V channels is a fairly young research topic and gained momentum in 2006, when the WAVE initiative and other vehicular applications raised the interest in vehicular communications. Before 2006, V2V channels were rarely investigated, e.g., [70]. Several V2V channel measurement campaigns were carried out since 2006 [6], [15]–[19], [25], [71], [72].

As mentioned in Section II-B until recently, the classical environments, *highway*, *urban*, *suburban*, and *rural*, were used for describing the scenarios. Further, the measurement vehicles were driving either in convoy or in opposite directions. Based on the literature, we summarize in the following important radio channel characteristics for these classical scenarios. Especially for V2V

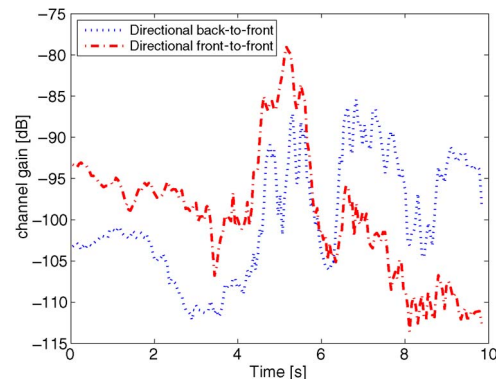


Fig. 11. Channel gain for back-to-front and front-to-front for a V2I channel.

communications, application-specific scenarios are of much higher interest, because the behavior of the radio channel differs significantly from the classical ones in specific scenarios. Therefore, we carried out a V2V radio channel measurement campaign [25] featuring scenarios for safety related applications, e.g., collision avoidance in a traffic congestion or at an intersection. Below, we analyze the APDP, channel gain, and rms delay spread of two selected scenarios.

1) *Highway*: A pathloss exponent of $n = 1.8 - 1.9$ on highways with light traffic was observed in [17], [23], [73], and [74]. The mean rms delay spread on the highway ranges from 40 to 400 ns [14], [15], [17], [72], [73] where the smaller delay spreads relate to a low traffic density [14]. In all V2V environments, the Doppler spreads tend towards higher values compared to conventional cellular channels, because the relative velocity between the Tx and the Rx can be higher and many significant scatterers are mobile. The mean Doppler spread was found to be approximately 100 Hz [17], [70], but Doppler spreads up to 1 kHz were also observed [72].

2) *Rural*: As in the highway environment, pathloss exponents of $n = 1.8 - 1.9$ were observed [74]. As a refinement to (1), a so-called break point model has been proposed [17]. This model specifies two pathloss exponents: $n = 1.8 - 1.9$ is valid up to the break point distance ~ 220 m and beyond that the higher pathloss exponent $n = 4$ is applied. These are in reasonable agreement with two-ray models [17], [74]. In the rural environment the lowest mean rms delay spreads of 20–60 ns [17], [72] were observed. The median Doppler spread was found to be approximately 100 Hz in [17] while Tan *et al.* [72] report a mean Doppler spread of 782 Hz.

3) *Suburban*: In the suburban environment, a break point model was found suitable, with a pathloss exponent of $n = 2 - 2.1$ at distances below 100 m and around $n = 4$ beyond that distance [18]. A mean rms delay spread of 104 ns was found in [15].

4) *Urban*: A pathloss exponent of $n = 1.6 - 1.7$ was observed in [17] and [23]. The measured mean rms delay spreads for the urban environment, 40–300 ns [14], [15], [17], [72], are comparable with those from the highway environment, though the rms delay spreads in [14] and [15] were doubled compared to the highway environment. The Doppler spreads of 30–350 Hz are lower compared to the highway and rural environments.

5) *Case Study 1—Intersection*: This scenario consists of a two-way intersection in Lund, Sweden, with one four-story building cornering the two perpendicular roads on which the vehicles are approaching. There is one lane in each direction and there is no other traffic during this

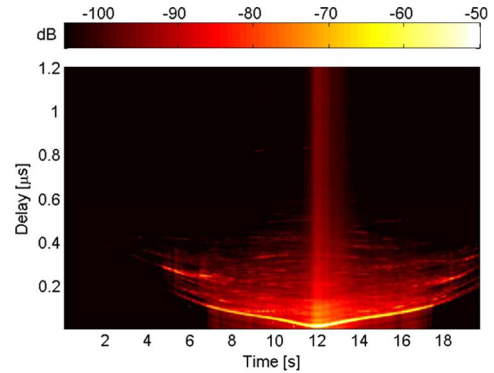


Fig. 12. APDP over the combined antenna pattern for the intersection scenario.

measurement run. Except for the cornering building, the area is more or less empty. The surrounding area consists only of a few distant one-story parking garages and some vegetation. Since there is no LOS between the vehicles before they enter the intersection and there are only a few scattering objects, low received power is expected. The measurements were conducted using a four-element uniform linear antenna array (ULA) integrated into a conventional automotive antenna housing, which was mounted on the rear part of the vehicle roof. Circular short-circuited patch elements with terrestrial coverage were applied in accordance to [33]. In order to increase the multipath resolution of the antenna from scatterers located along the road, the ULA was oriented perpendicular to driving direction featuring a $\lambda/2$ interelement spacing. While the four individual antennas exhibit sectoral coverage, its sum pattern was specifically designed to provide almost omnidirectional coverage in azimuth. Metallic director elements were integrated into the antenna compartment to improve the beam coverage. The antenna housing was exclusively equipped with the 5.9-GHz ULA while antennas for additional radio services were unpopulated from this mounting space. Fig. 12 shows the APDP over the combined antenna pattern, explained in the case study of Section II-D, of the intersection scenario. In Fig. 13, the channel gain for two selected single links (front-to-front and back-to-back antenna pattern) are shown. The front beam pattern faces the driving direction whereas the back beam pattern faces the rear direction. The depicted Rx beam pattern orientation in Fig. 9 is also valid for the Tx vehicle. These two links are selected, because they exhibit the two extreme channel gains. While the vehicles are approaching each other, the front-to-front channel gain is the strongest among all others whereas it is the lowest one after the vehicles passed each other, and conversely for the back-to-back channel gain. In Fig. 14, the rms delay spread of the intersection scenario is shown, which is compared with the traffic congestion scenario in Section II-E7.

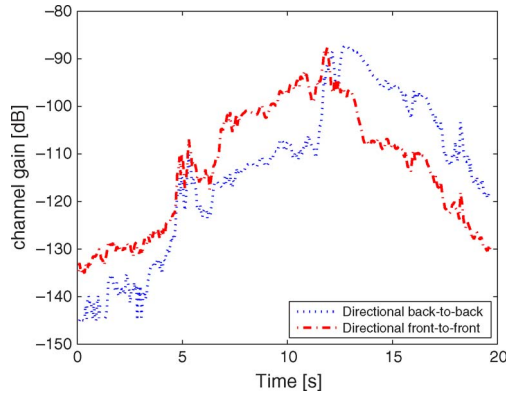


Fig. 13. Channel gain for directional back-to-back and front-to-front antenna pattern for the traffic congestion scenario.

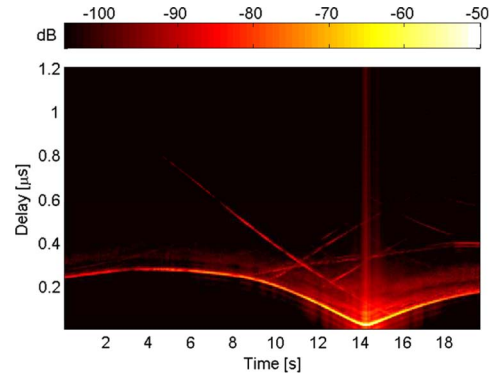


Fig. 15. APDP over the combined antenna pattern for the traffic congestion scenario.

6) *Case Study 2—Traffic Congestion:* The Tx vehicle is stuck in a traffic congestion on the right lane of a highway with two lanes in each direction in the vicinity of Lund, Sweden. The Rx vehicle starts approximately 600 m behind the Tx by overtaking a large truck. Afterwards the Rx vehicle is overtaking the Tx vehicle with a speed up to 60 km/h \approx 37.3 mph \approx 16.7 m/s. There are several traffic signs above and next to the highway and a bridge runs across. Dominating multipath components from moving and static objects in the vicinity of the two measurement vehicles are expected. Results of the APDP and Doppler spectral density (DSD) and a more detailed description of this scenario are presented in [25].

Fig. 15 shows the APDP over the combined antenna pattern of this congestion scenario. The MPCs stem from scattering at trucks, traffic signs, and bridges. All are time varying over the whole measurement duration. In Fig. 16, the channel gains for the same two single links as for the intersection scenario are shown. We chose the same single links, in order to show the different behavior of the

channel gain of single links in different scenarios. Fig. 17 shows the rms delay spread for the traffic congestion scenario.

7) *Comparison of the Two Scenarios:* First, we discuss the APDP of both scenarios: We observe that in the case of the congestion scenario the LOS path is present during the whole measurement duration, even if it is blocked during the earliest 4 s of the measurement. In the intersection scenario, scattered paths occur only shortly before the LOS becomes unobstructed between the Tx and the Rx. This means that it is not possible to transmit a signal much before the LOS occurs, due to the absence of scattering objects in the vicinity.

Next, we compare the single link channel gains of both scenarios: We see that the dynamic range of the channel gain over time is much higher in the case of the intersection scenario (intersection: \sim 45 dB, traffic congestion: \sim 30 dB). The main reason is a lack of significant multipath contributions at the intersection before the LOS becomes unobstructed at approximately 6.5 s. The channel gain of

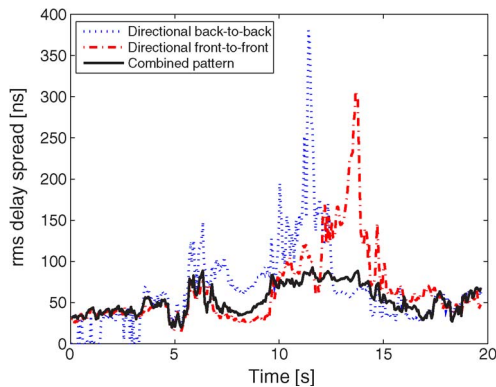


Fig. 14. RMS delay spread over the combined antenna pattern as well as for directional back-to-back and front-to-front antenna pattern for the intersection scenario.

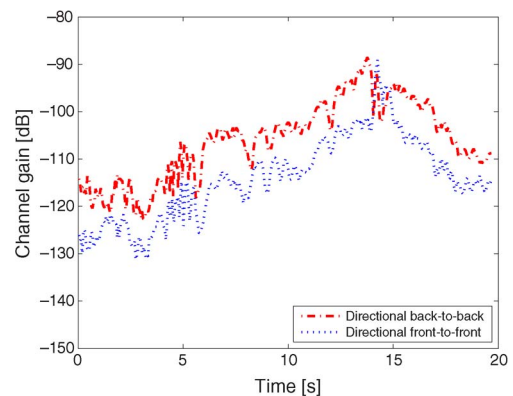


Fig. 16. Channel gain for directional back-to-back and front-to-front antenna pattern for the traffic congestion scenario.

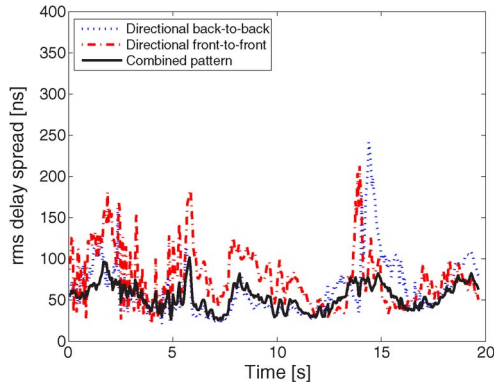


Fig. 17. RMS delay spread over the combined antenna pattern as well as for directional back-to-back and front-to-front antenna pattern for the traffic congestion scenario.

the front-to-front link in the intersection scenario is larger than the channel gain of the back-to-back link before the vehicles are passing and *vice versa* when the vehicles are leaving.

In the congestion scenario, the channel gain of the back-to-back link is always larger than the front-to-front gain, except for a very short peak after the vehicles passed. To ensure dependable vehicular links and robust connectivity, the use of diversity techniques and link adaptation is crucial.

The mean values for the time-varying rms delay spread (Figs. 17 and 14) for the combined antenna patterns are for both scenarios about 50 ns. Even though the mean values for both scenarios are quite similar, we observe a more peaky profile for the intersection scenario. One peak is at 11.4 s for the back-to-back link and at 13.7 s for the front-to-front link. These peaks coincide with the shadowing of the LOS component and the subsequent MPCs are strong enough to increase the rms delay spread. A similar phenomenon, however less pronounced, can be observed for the congestion scenario at 13.9 and 14.4 s for both shown links.

F. Vehicular Channel Models

For system performance evaluation by simulation [75] and the analysis of novel signal processing algorithms, radio channel models are needed, which allow to compute the input–output behavior of vehicular propagation channels. Most importantly, pathloss, delay and Doppler spread, fading statistics, and the channel’s nonstationarities need to be modeled. For vehicular channels, we distinguish three types of radio channel models: tap delay models, ray-based models, and geometry-based stochastic models.

1) *Tap Delay Models*: In tap delay models, the impulse response of the channel is modeled with components at certain delays (“taps”), hence the channel is modeled by

a so-called tapped delay line (TDL). The average power of the taps is assumed to decay exponentially in delay lag. Fading is implemented by varying the amplitude of each tap over time according to specified fading distributions. Depending on the fading distributions of the taps, the channel can be modeled with a strong LOS connection between the Tx and the Rx (leading to Ricean fading), or without LOS (Rayleigh fading). Each tap may feature an individual Doppler spectrum. Such a model was proposed and parameterized for IEEE 802.11p by Acosta-Marum *et al.* [19], [76].

The statistics of vehicular channels may change over time, because the (short-term-averaged) power associated with a reflector fluctuates and the delays of the channel taps drift as the distances between the Tx, the Rx, and reflectors vary (violation of “wide-sense stationarity” assumption). Further, the channel may show correlated fading for different delays due to several MPCs interacting with one-and-the-same object (violation of “uncorrelated scattering” assumption). These are specific characteristics of vehicular channels, which are not adequately reproduced in standard TDL models though remedies for this have been suggested, e.g., in [14].

2) *Ray-Based Models*: For this approach, a highly accurate description of the electromagnetic propagation environment is mapped into a software model. This includes detailed modeling of all objects affecting the wave propagation (e.g., vehicles, buildings, the road itself, traffic signs, foliage, other cars, etc.). Further, the scattering behavior of these objects needs to be represented accurately. After the software model is generated, wave propagation is simulated by determining all possible paths from the Tx to the Rx. This provides a site-specific, very realistic simulation of the propagation channel. Such models provide (and require) a large amount of map details and they tend to high computational complexity. Pioneering work on ray-based models in general, and for vehicular channels in particular, has been done in [70], [77], and [78], where wave propagation was modeled along a street.

3) *Geometry-Based Stochastic Models*: For geometry-based stochastic models (GSCMs), the geometry of the propagation environment is randomly generated according to specified statistical distributions. For vehicular channels, several models have been proposed with randomly placed scatterers in circles or ellipses around the vehicles [79]–[84].

This model class does not target the accurate computation of the channel impulse response realizations [85]. Dedicated vehicular radio channel measurements at 5 GHz showed that the main contributions in the channel impulse response are: LOS, deterministic scattering, and diffuse scattering components. The LOS component has high gain as long as there is a direct path from the Tx to the Rx. The LOS component’s gain decreases whenever an interacting

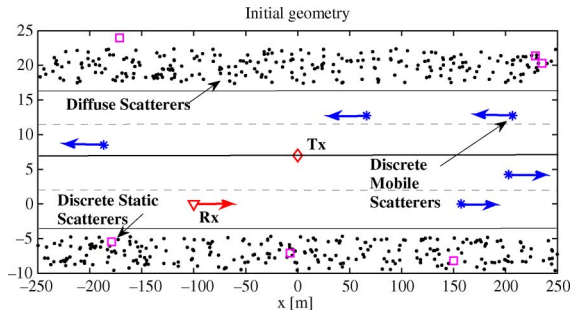


Fig. 18. Geometry-based stochastic vehicular channel model [85]: exemplary random scatterer distribution over 500 m.

object obstructs the direct path (shadowing). The diffuse scattering contribution, stemming from surrounding buildings, other structures along the road, or foliage, forms a fairly large fraction of the overall channel gain. For these reasons, we proposed a geometry-based stochastic channel model in [85]. This model is parameterized from vehicular measurements at 5.2 GHz [69] and models all mentioned features.

An example for a typical infrastructure-to-vehicle scenario along a highway is shown in Fig. 18. A roadside Tx and a vehicular Rx are deterministically placed. Then, mobile discrete (MD) scattering objects, static discrete (SD) scattering objects, and diffuse (D) scatterers at both sides of the road are randomly generated. The MD scatterers symbolize other cars driving along the road, while the SD scatterers represent traffic signs. The diffuse scattering wall models the foliage along the highway. The speed of the MD scatterers is stochastically assigned from a distribution with mean 90 km/h \approx 56 mph \approx 25 m/s and a standard deviation of 2 km/h \approx 1.24 mph \approx 0.56 m/s, to reflect a situation on a real highway. The velocity of the Rx is set to 100 km/h \approx 62 mph \approx 28 m/s.

The time-varying channel transfer function is computed as a superposition of all the discrete propagation paths in this simulated environment. A computationally advantageous implementation of this model is discussed in [86].

III. IMPLICATIONS FOR WIRELESS SYSTEMS

In order to support vehicular communications, the IEEE 802.11 standard [8] has been amended by Task Group P (TGp). The IEEE 802.11p amendments makes use of the orthogonal frequency division multiplexing (OFDM) physical layer (previously specified in the IEEE 802.11a standard [87]), and the quality-of-service extension on the medium access control (MAC) layer (also known as IEEE 802.11e). Both standards, IEEE 802.11a and IEEE 802.11e, were initially designed for indoor and nomadic wireless local area networks (WLAN). The IEEE 802.11p specifies a

set of parameters for the physical (PHY) layer, addressing vehicular scenarios.

A. General Guidelines for OFDM System Design

The IEEE 802.11p standard is based on OFDM [88], [89]. OFDM is a modulation technique where the overall transmission bandwidth B is subdivided into N orthogonal subcarriers with bandwidth B/N . Each subcarrier is subject to frequency flat fading, allowing for simple channel equalization at the receiver side. To avoid intersymbol interference, i.e., symbols overlapping due to multipath, OFDM implements a specific form of guard period, the cyclic prefix. The cyclic prefix is a copy of the last G samples from the end of the OFDM symbol. To implement OFDM, a discrete Fourier transform (DFT) is computed at both Tx and Rx sides. Due to the efficient implementation of the DFT by means of the fast Fourier transform, OFDM is very well integrated into current chip sets.

For the OFDM system design two basic parameters of the wireless channel must be taken into account: the (maximum) excess delay τ_{\max} and the Doppler spread f_D (see Section II).

The (maximum) excess delay sets a limit on the maximum data rate that can be used without equalizer, or similarly it determines the minimum duration of the cyclic prefix in OFDM systems

$$\tau_{\max} < \frac{G}{B}. \quad (4)$$

The Doppler spread determines the minimum subcarrier spacing in OFDM systems before the onset of intercarrier interference, due to loss of subcarrier orthogonality [90]

$$f_D \ll \frac{B}{N}. \quad (5)$$

As additional constraint the spectral efficiency

$$\eta = \frac{N}{N + G} \quad (6)$$

shall be as large as possible.

For coherent detection, channel state information (CSI) is required. To obtain CSI, current OFDM standards rely on known pilot symbols that are interleaved with the data in the OFDM time-frequency grid. For the system design it is crucial to place the pilot symbols in the OFDM time-frequency grid according to the maximum excess delay and the Doppler spread of the wireless communication channel. The maximum excess delay determines how dense pilot symbols must be transmitted in frequency

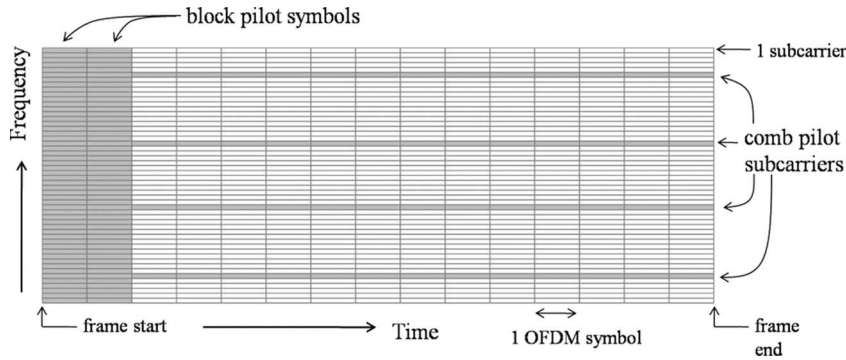


Fig. 19. Pilot allocation in IEEE 802.11p.

domain, and the maximum pilot spacing Δ_f (number of subcarriers) will satisfy

$$\Delta_f \leq \frac{N}{\tau_{\max} B}. \quad (7)$$

The Doppler spread determines how dense pilot symbols must be placed in time. The maximum spacing Δ_t (number of OFDM symbols) will satisfy

$$\Delta_t \leq \frac{B}{2f_D(N + G)}. \quad (8)$$

Specific choices of OFDM parameters allow for a wide range of applications from broadcasting [90]–[94] to cellular [95], WLAN [87], and vehicular connectivity [8].

B. IEEE 802.11p System Performance

The IEEE 802.11p standard was derived from IEEE 802.11a [87], [96] with specific modifications for vehicular scenarios. Particularly, the bandwidth of 802.11p was reduced to 10 MHz to ensure that the cyclic prefix length of $G = 16$ samples corresponds to a larger tolerable excess delay, namely up to $1.6 \mu\text{s}$ (corresponding to 480 m propagation distance). From a total of $N = 64$ subcarriers, only 52 are utilized due to guard band requirements. Eight different coding and modulation schemes allow for data rate adaptation ranging from 3 to 27 Mb/s.

Traffic telematics applications require a dependable vehicular connectivity.⁴ In the following sections, we review the 802.11p performance under realistic channel conditions.

⁴In the early drafts of 802.11p [76], minimum performance requirements were specified. In the final version [8], such requirements are missing.

1) *Channel Estimation Techniques*: The system performance of the 802.11p standard is largely determined by the channel estimator and equalizer in the receiver. We investigate the system performance for estimation and equalization techniques that are implementable in chip sets at moderate complexity. To reuse the chipset design, the 802.11p pilot pattern is identical to the already established 802.11a pilot pattern. This pilot pattern is well designed for nomadic indoor usage, but less so for vehicular scenarios where the channels are jointly time-frequency selective. This leads to a performance loss if too naive channel estimators are used.

The IEEE 802.11p pilot pattern considers two kinds of pilots: 1) block pilots [8] as shown in Fig. 19.

All 52 subcarriers of the first two OFDM symbols are dedicated to pilots. In the remaining OFDM symbols, only four subcarriers contain pilots throughout the whole frame duration. Based on this pilot pattern, we investigate two types of common channel estimators: the block and the block-comb channel estimator, respectively [97].

- *Block-type channel estimator*: An estimate of the channel is calculated from the block pilots, only. The estimated channel coefficients are used for the whole frame, hence no time variation is taken into account. The block least square (B-LS) estimator [98]–[100] is defined in [97, (1)]. It is the commercial off-the-shelf (COTS) choice for chip set implementation.
- *Block-comb channel estimator*: First, the time correlation function is estimated using the comb pilots. Subsequently, linear minimum mean square error (MMSE) filtering for each subcarrier is applied [97, (3) and (4)]. This structure requires higher complexity than the B-LS estimator for allowing time variance of the channel.

These techniques have been used in other communication systems with good results [98]–[100], [102], [103]. The operation region of the BC-MMSE (“COTS”) estimator using the 802.11p pilot pattern is shown schematically in Fig. 20. Acceptable performance is expected for short

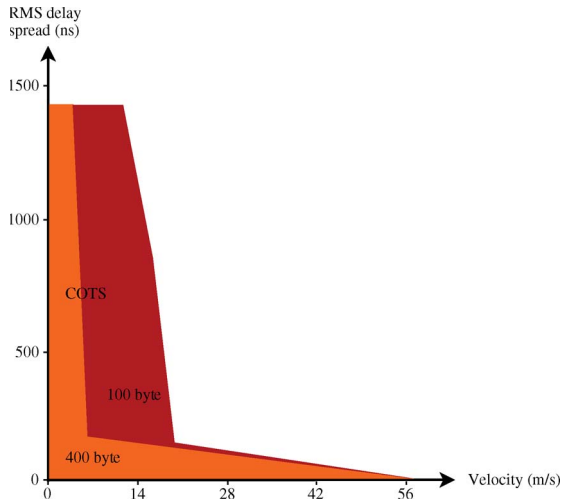


Fig. 20. Operation region for BC-MMSE estimator using 802.11p pilots [101] with parameters: 3 Mb/s, 100- and 400-B packet length, packet error ratio < 10%, -78-dBm receive power, 10-MHz bandwidth, 5.9-GHz carrier frequency. The maximum velocity of 56 m/s corresponds to approximately 200 km/h \approx 124 mph.

block lengths, as well as for channels with either short delay spread and high Doppler spread, or high delay spread but low Doppler spread. Conversely, in NLOS conditions with Doppler spread $f_D > 500$ Hz and maximum excess delay $\tau_{\max} > 400$ ns performance losses are inevitable.

2) Numerical Simulation: We implemented an IEEE 802.11p compliant PHY layer simulation environment in MATLAB. In the simulations, data blocks are randomly generated and transmitted with coding and modulation scheme 3 at 6 Mb/s. This scheme uses quadrature phase shift keying and a convolutional code with constraint length 7 and coding rate 1/2.

The transmission was simulated using two different channel models for a vehicle driving at $v = 100$ km/h \approx 28 m/s \approx 62 mph: 1) a Rayleigh fading channel with an exponentially decaying power delay profile with $\tau_{\text{rms}} = 400$ ns and Clarke Doppler spectrum [53] for each tap modeling a NLOS scenario (similar to the “RTV-Expressway” TDL model described in [19] [cf. Section II-F1]); 2) the (nonstationary) GSCM [85] (cf. Section II-F3), implementing the scenario in Fig. 18. The channel realizations are generated randomly for a distance of 100 m to the APs. New scatterer and vehicle realizations are generated for each individual frame.

In Figs. 21 and 22, we plot the bit error rate (BER) versus SNR for both models, respectively. Error floors are obvious in both error curves at high SNRs. This implies that an error-free link is out of reach for COTS channel estimators (regardless of the SNR). Due to the stronger LOS component in the GSCM, the effective delay spread of the channel is smaller than in the Clarke NLOS model.

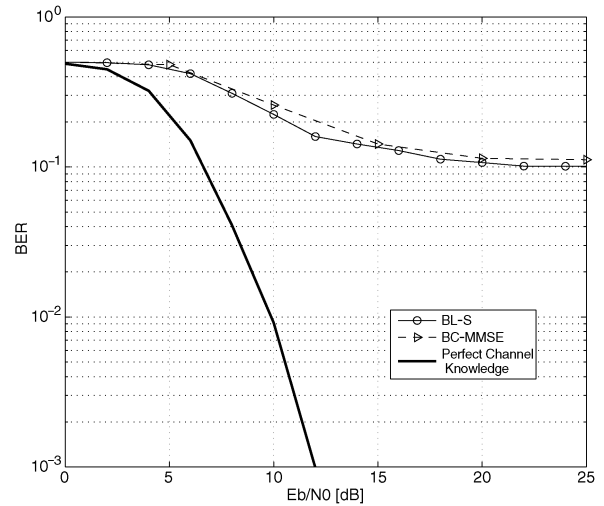


Fig. 21. BER versus SNR for exponentially decaying PDP and Jakes Doppler spectrum in NLOS situation (model according to [19]).

Hence, the channel estimator performance for the first case is worse due to having four pilot subcarriers only.

Since the IEEE 802.11p pilot pattern was designed for low complexity receivers in nomadic indoor environments, a degraded performance in highly mobile environments is no surprise when reusing the original low-complexity chip design. A low packet error rate in NLOS scenarios is crucial for safety-related scenarios, and IEEE 802.11p receivers of higher complexity will be required.

Further, the use of multiple Rx antennas may improve the performance significantly [34], [35], [104], [105]. Multiple antennas provide the appropriate radio interface for interference mitigation, link reliability, and network

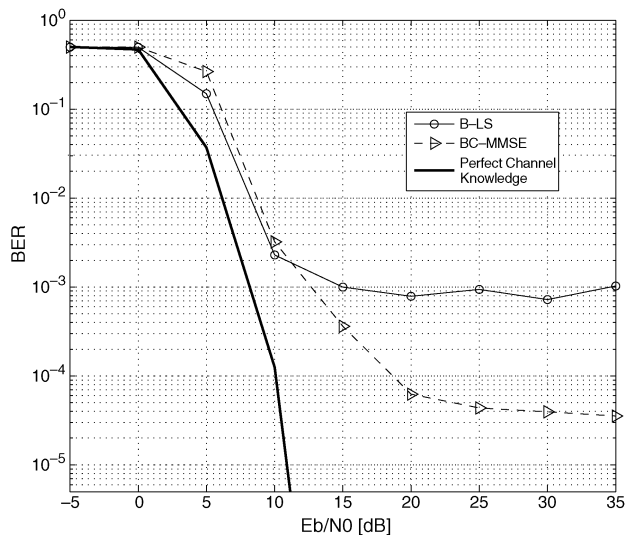


Fig. 22. BER versus SNR for a nonstationary model with strong LOS component (model according to [85]).

scalability. Many multiple antenna techniques are based on spatial diversity concepts, but also polarization diversity antennas [106] are of interest for fading mitigation, depending on the fading statistics of the channel. The delay and Doppler spreads of the channel are reduced by these measures, thus improving system performance. In the long run, Rx improvements will be enabled by a thoughtful evolution of the IEEE 802.11p standard with a redesigned pilot pattern.

C. Transmission Experiment

Apart from numerical simulations, we also carried out a V2I measurement campaign with an IEEE 802.11p prototype system on a highway in Austria.

Previously, measurements with standard IEEE 802.11a/b/g equipment in V2V and V2I scenarios showed that the vehicle distance and availability of LOS are highly significant performance factors [107]. The authors observed a higher number of retransmissions for larger packet sizes and a reduced communication range for higher order modulation schemes. The work in [108] investigates the performance of IEEE 802.11a with various bandwidths and compares measured V2V channel parameters with critical parameters of IEEE 802.11a/p. The most critical parameter was found to be the packet length, because it is longer than the coherence time of the radio channel, especially when using the smaller bandwidth of 10 MHz in IEEE 802.11p compared with 20 MHz in IEEE 802.11a. In [109], the modifications of IEEE 802.11p related to IEEE 802.11a, in order to make the new standard IEEE 802.11p more robust in vehicular scenarios, are presented. Several investigations deal with simulation-based performance evaluations, e.g., [110] and [111]. Eichler [110] concluded that in dense traffic scenarios IEEE 802.11p cannot ensure time-critical message dissemination, because of long MAC queues and high end-to-end delays. In [111], simulations show that 90% of successful communications were conducted at a distance of 750 m. In the United States, significant work was done by Eriksson and Balakrishnan [112], discussing improvements to the communication protocol for speeding up the connection time. Another vehicular testbed was presented in [113], which enables radio and MAC layer performance assessment, the efficient use of multiple 802.11p channels (control and data), network protocol testing, and experimental validation of algorithms. A preliminary experiment on a university campus showed an average frame loss rate of 0.09 for a video streaming application.

1) *Measurement Setup*: In our V2I measurements, we investigated the PHY layer of IEEE 802.11p downlink broadcast with a *transparent* MAC layer (i.e., without retransmissions). This investigation of the PHY layer in real-world V2I scenarios allows us to identify strengths and room for future PHY improvements to enable dependable connectivity.

a) *Experiment setup*: In July 2009, we carried out the trials on a highway in mountainous terrain, as part of the REALSAFE project [20]. The measurement campaign's goal was to characterize the average downstream packet broadcast performance for a vehicle passing two roadside units (RSUs). As test platforms, we used three nodes of the cooperative vehicle-infrastructure system (CVIS) platform [114], implementing the IEEE 802.11p draft standard. The radio module is equipped with a GPS receiver for onboard unit (OBU) location logging and providing an accurate time stamp to both the OBU and the RSUs.

Two RSUs were installed at fixed locations on the highway with different antenna heights and configured as IEEE 802.11p transmitters continuously transmitting data packets with random data. The RSUs were configured for several experiments with different packet lengths and data rates. The transmit power was set to 15.5 dBm (equivalent isotropically radiated power). We used vertically polarized monopoles as RSU antennas. The distance between both RSUs was chosen large enough for avoiding interference.

The OBU was configured as IEEE 802.11p receiver with logging capabilities. As OBU antenna, the CVIS vehicle antenna [114] was used. Its beam pattern was specifically designed to provide omnidirectional coverage with linear vertical polarization in azimuth including mutual coupling between individual antennas located in the same multi-standard antenna compartment. Vehicular integration effects were not taken into account for beam pattern optimization. The antenna module was magnetically mounted on the rear part of the vehicle roof and centered with respect to driving direction. For documentation, we used two video cameras. While the RSUs were transmitting frames continuously, the OBU received frames only when being in the coverage area. At the Rx, we counted the correctly decoded frames and logged the received signal strength indication (RSSI) values, frames numbers, and associated time stamps.

b) *Measurement scenario*: As measurement scenario, we chose the A12 highway in Tyrol, Austria. There are two lanes in each direction. The lane divider consists of a waist-high concrete wall followed by bushes of the same height. The measurements were carried out in real traffic conditions for both driving directions (west and east) separately.

We investigated two RSU mounting positions. 1) The RSU antenna was mounted on a metal pillar on top of a highway gantry, 7.1 m above the highway level (see Fig. 23). This scenario is termed "high RSU." 2) The antenna is mounted next to the gantry on a snow-protection wall. The antenna height is 1.8 m above the road level (see Fig. 24). This second scenario is denoted as "low RSU."

2) *Measurement Results*: As key performance indicator, we used the frame-success ratio (FSR), which is defined as the number of correctly decoded frames divided by the number of total transmitted frames during a specified time interval. We define the *achievable range* for the RSU on the

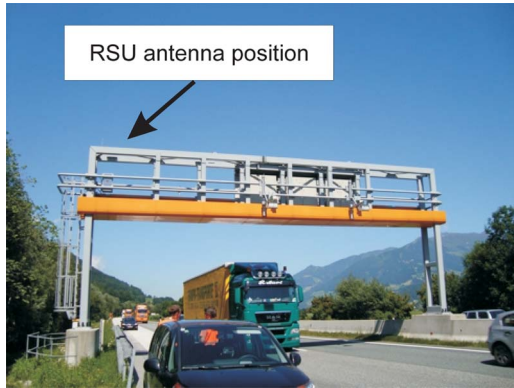


Fig. 23. Measurement scenario “high RSU” including RSU antenna position.

interval where the FSR is permanently above a given threshold. Fig. 25 illustrates this definition of achievable range. The FSR is plotted for various distances between the vehicle and the RSU. The colors indicate the three different measurement runs. Close to the RSU, the FSR is generally high, while showing a steep drop at some distance. The strong fluctuations are due to various environmental effects. Below, we discuss the effects of the environment, traffic, and different coding and modulation schemes on the system performance.

a) *Environment effects:* We analyzed irregularities in the FSR and drew conclusions by visual inspection of the measurement videos and the topology.

First, an unexpected throughput drop caused by propagation effects occurred consistently at a distance of 300 m east of the high RSU [20] as shown in Fig. 25. We hypothesize that this throughput drop was caused by LOS blocking and the Rx hardware was unable to equalize rich multipath channels at low SNR.

Second, we observed an unexpected coverage at a very large distance of 0.7–1.2 km east of the (low-height) RSU



Fig. 24. Measurement scenario “low RSU.”

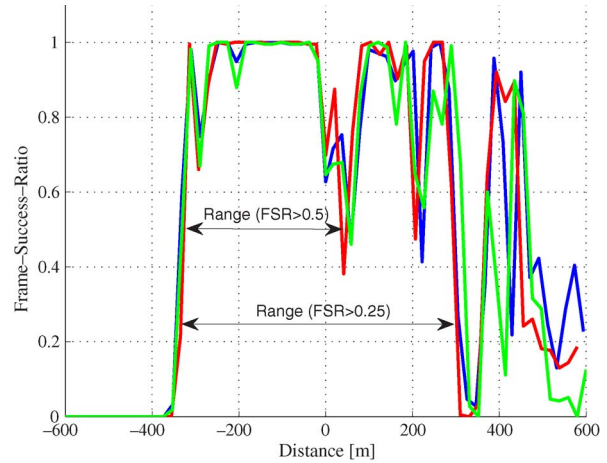


Fig. 25. Definition of achievable range in the presence of FSR fluctuations. The RSU is placed at a distance of 0 m.

as seen in Fig. 26. This effect is due to a bridge over the highway with metal railing. The (vertical) metal rails act as secondary linear antenna array, where the main lobe of its antenna pattern is directing onto the highway. This can also be interpreted as multiple reflections off the metal rails, which have constructive interference along the road. For site planning, this long-range coverage must be considered as interference for the adjacent IEEE 802.11p cells; we recommend mitigation by using additional wave absorbers at the bridge railings.

b) *Road traffic effects:* Road traffic has a severe influence on the FSR. Depending on the traffic situation, moving vehicles that block the LOS between the Tx and the Rx can degrade the performance significantly. Fig. 27 depicts a LOS blocking effect that we observed for several measurement runs close to the low RSU. The FSR of

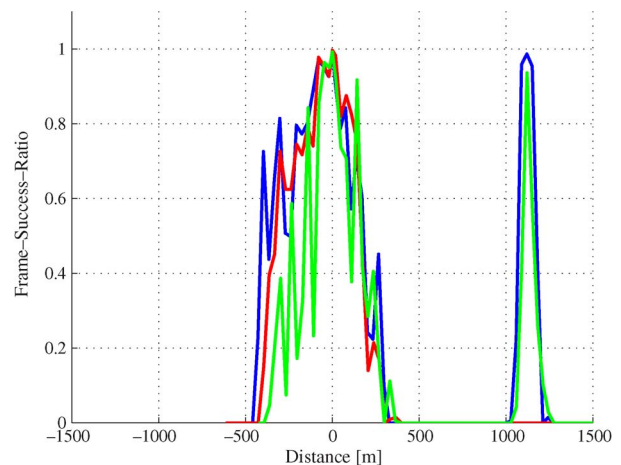


Fig. 26. Bridge effect: coverage at 1200-m distance from RSU resulting from radio wave focusing by bridge railing.

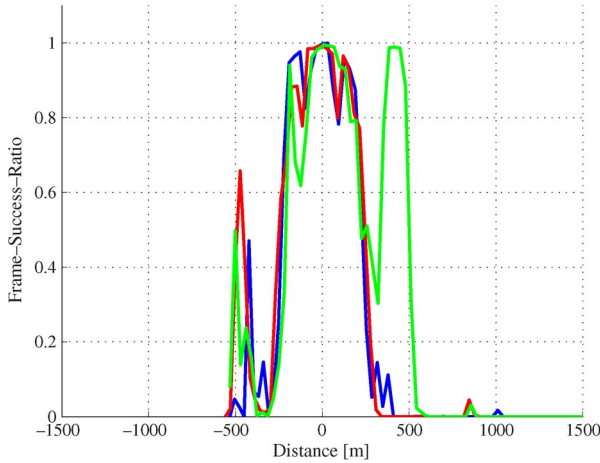


Fig. 27. Road traffic effect: three measurement runs in the same environment (different colors) lead to differing FSR due to road traffic. Note the coverage loss at 400-m distance from the RSU.

different runs varies significantly where the blocking occurs (e.g., at a distance of 400 m in Fig. 27). These effects demonstrate the peculiar large-scale fading characteristics of vehicular environments. Clearly, LOS blocking is much more severe at the low RSU since the antenna position is unfavorable. At the high RSU, blocking did not lead to such severe effects. For this reason, we recommend to use high RSU antenna positions for V2I communications.

c) *Modulation and coding scheme test:* Fig. 28 shows the achievable ranges for a packet length of 200 B and a vehicle speed of 33.3 m/s \approx 120 km/h \approx 75 mph over all configurable data rates in IEEE 802.11p (3–27 Mb/s). Since higher SNR is required for higher data rates, we observe a decreasing range with increasing data rate.

Focusing on the RSU antenna height, the ranges for driving west and east are very similar for the high RSU. However, for the low RSU, the low antenna position was

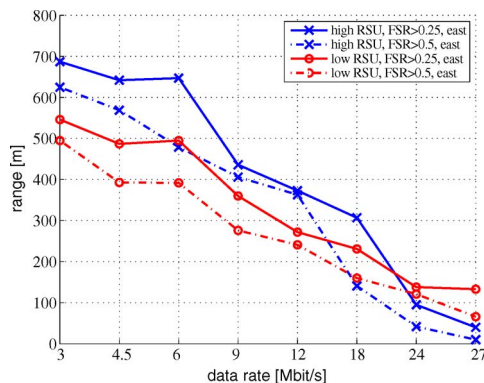


Fig. 28. Range versus data rate: higher data rates require stronger receive signal powers. A high mounting of the RSU leads to better coverage.

again unfavorable for driving on the opposite lane (going east). For this reason, the achievable range shows a large difference compared to the high RSU.

An interesting effect occurs at high data rates, where the low RSU position outperforms the high RSU position in terms of range. The reason for this is that due to the antenna pattern, the high-RSU antenna has bad coverage below its gantry. The signal quality only starts increasing beyond a certain distance from the gantry. This is also reflected in Fig. 25, where a drop in throughput can be noticed at distance 0. In contrast, the low-RSU antenna provides good coverage for short ranges in its vicinity. Thus, the achievable range is larger for high data rates.

IV. OPEN ISSUES AND SUGGESTIONS FOR FUTURE RESEARCH

In this paper, we have reviewed current research in V2I and V2V propagation channels and their impact on system design. In the following, we summarize the key insights, and suggest future research directions.

The propagation conditions in particular for V2V communications are influenced by the antennas and their placement on the vehicle. The roof of the vehicle can strongly influence the antenna pattern; if the antenna is placed on a backward-slanted roof it has difficulties “seeing” vehicles in front of it. Multiple antennas are deployed either in the form of multibeam antennas, or as linear arrays.

Generally, V2I channels show great similarity to “conventional” cellular propagation channels. Deployment scenarios that show unique propagation conditions for V2I are infrastructure in tunnels and on gantries/overpasses over highways or when the infrastructure is at very low height. V2V scenarios have historically been categorized into highway, rural, urban, and suburban environments. However, we demonstrated in this paper that application-specific scenarios, which are not explicitly covered by the above categorization, have even greater importance. In particular, the details of intersections and lane merging should be carefully modeled, as they affect safety-critical applications.

For both V2V and V2I channels, key properties are 1) pathloss and fading statistics; 2) temporal variance; and 3) delay spread. Concerning pathloss and fading, it is noteworthy that the coverage region of a transmitter is *not* a circle around the transmitter, but rather a complex-shaped and even noncontiguous region. Furthermore, the region over which the transmitter provides coverage is smaller than the region in which it creates interference. Due to the high speeds involved, V2V and V2I channels show strong time variance (the channel state changes) and nonstationarity (the channel statistics change). These effects are more pronounced for cars approaching each other or approaching intersections, while they are less severe for vehicles driving in convoys, or V2I communications. Finally,

we found that antenna patterns have a strong impact on the delay spread; with a suitable choice of antenna patterns (e.g., by beam selection) delay spreads can become much shorter than previously reported in the literature.

The channels are simulated efficiently by both GSCM and TDLs. Possible nonstationarities are implicitly modeled by GSCMs, while TDLs have to be modified to provide time-varying tap locations and statistics. Ray-based models, on the other hand, provide accurate results for specific locations and surrounding structures.

As future topics for research in the channel area, the following seem especially pressing: 1) obtaining larger number of samples for all environments, in order to increase statistical significance; 2) quantify the difference of channels in the same environment (e.g., highway) in strongly contrasting countries; 3) analyze the impact of trucks or other shadowing objects in particular on V2V channels; 4) analyze directional channel characteristics, in particular for V2V channels, since for those the traditional mapping between Doppler shift and directions is not unique; 5) experimental investigation of the impact of antenna mounting on the car; and 6) developing TDL with time-varying tap locations and statistics.

Another key conclusion of our paper is that any system design has to be adapted to the properties of the propagation channels, in particular to the time-varying joint Doppler and delay spread.

Currently, the dominating standard for V2V communications is IEEE 802.11p, which is derived from the popular 802.11a (WiFi) standard. There is potential for future improvements: A modified pilot pattern would allow to reduce receiver complexity. Multiantenna transmitters (possibly similar to those foreseen in high-throughput

WiFi, IEEE 802.11n) would increase diversity and thus enhance reliability of the links. Further, multiantenna transmitters and receivers could mitigate cochannel interference by beamforming and/or increase data rate through spatial multiplexing. Another topic that has great impact on the overall performance is the MAC layer [115].

Simulations with simple receivers using COTS components showed an error floor, which motivates improved receiver architectures. Improved channel estimation can decrease or eliminate the error floor. The experiments motivated to place APs as high as possible on gantries. As a general rule, the site-specific deployment of the APs will have a major impact on the coverage and reliability of infrastructure-based communications.

Overall, the field of vehicular propagation channels and system design continues to provide fascinating and worthwhile challenges. ■

Acknowledgment

The authors would like to thank P. Fuxjäger, E. Hasenleithner, and H. R. Fischer for their software hacks of the CVIS platform as well as R. Tresch, A. Alonso, D. Smely (Kapsch TrafficCom), and P. Meckel (ASFINAG) for their support in experiments. They would also like to thank ERTICO and Q-FREE for granting the use of the CVIS platform and for technical support, and SMARTEQ for supplying the RSU antennas. The Federal Ministry for Transport, Innovation, and Technology of Austria (BMVIT) is acknowledged for granting a test license in the 5.9-GHz band. The authors would like to thank the reviewers for their constructive comments that helped to substantially improve this paper.

REFERENCES

- [1] *Intelligent Transport Systems (ITS): Vehicular Communications; Basic Set of Applications; Definitions*, ETSI TR 102 638, V1.1.1, Jun. 2009.
- [2] P. A. Bello, "Characterization of randomly time-variant linear channels," *IEEE Trans. Commun. Syst.*, vol. 11, no. 4, pp. 360–393, Dec. 1963.
- [3] R. Thomä, D. Hampicke, A. Richter, A. Schneider, G. Sommerkorn, U. Trautwein, and W. Wirtzner, "Identification of time-variant directional mobile radio channels," *IEEE Trans. Instrum. Meas.*, vol. 49, no. 2, pp. 357–364, Apr. 2000.
- [4] G. Matz, A. Molisch, F. Hlawatsch, M. Steinbauer, and I. Gaspard, "On the systematic measurement errors of correlative mobile radio channel sounders," *IEEE Trans. Commun.*, vol. 50, no. 5, pp. 808–821, May 2002.
- [5] R. Thomä, M. Landmann, A. Richter, and U. Trautwein, "Multidimensional high-resolution channel sounding," in *Smart Antennas—State-of-the-Art*, vol. 3, T. Kaiser, Ed. Cairo, Egypt: Hindawi, 2006, pp. 241–270, ser. EURASIP Book Series on Signal Processing and Communications.
- [6] C.-X. Wang, X. Cheng, and D. I. Laurenson, "Vehicle-to-vehicle channel modeling and measurements: Recent advances and future challenges," *IEEE Commun. Mag.*, vol. 47, no. 11, pp. 96–103, Nov. 2009.
- [7] A. F. Molisch, F. Tufvesson, J. Karedal, and C. F. Mecklenbräuker, "A survey on vehicle-to-vehicle propagation channels," *IEEE Wireless Commun. Mag.*, vol. 16, no. 6, pp. 12–22, Dec. 2009.
- [8] *IEEE P802.11p-2010: Part 11: Wireless LAN Medium Access Control (MAC) and Physical Layer (PHY) Specifications: Amendment 6: Wireless Access in Vehicular Environments*, Jul. 15, 2010, DOI: 10.1109/IEEESTD.2010.5514475.
- [9] *Commission Decision on the Harmonised Use of Radio Spectrum in the 5875–5905 MHz Frequency Band for Safety-Related Applications of Intelligent Transport Systems (ITS)*, 2008/671/EC, Aug. 2008.
- [10] *European Profile Standard for the Physical and Medium Access Control Layer of Intelligent Transport Systems Operating in the 5 GHz Frequency Band*, ETSI ES 202 663, Final Draft v1.1.0, Nov. 2009.
- [11] *Intelligent Transport Systems—Communications Access for Land Mobiles (CALM)—M5*, ISO/FDIS 21215, Stage 50.00, Apr. 14, 2010.
- [12] *Car 2 Car Communication Consortium*. [Online]. Available: <http://www.car-to-car.org/>
- [13] M. Fujise, "Communications policy and ITS in Japan," in *Proc. 9th Int. Conf. ITS Telecommun.*, Lille, France, Oct. 20–22, 2009. [Online]. Available: <http://itst2009.inrets.fr/keynotes.htm>
- [14] I. Sen and D. Matolak, "Vehicle—Vehicle channel models for the 5-GHz band," *IEEE Trans. Intell. Transp. Syst.*, vol. 9, no. 2, pp. 235–245, Jun. 2008.
- [15] O. Renaudin, V. M. Kolmonen, P. Vainikainen, and C. Oestges, "Wideband MIMO car-to-car radio channel measurements at 5.3 GHz," in *Proc. IEEE Veh. Technol. Conf.*, 2008, DOI: 10.1109/VETEFC.2008.65.
- [16] A. Paier, J. Karedal, N. Czink, C. Dumard, T. Zemen, F. Tufvesson, A. Molisch, and C. F. Mecklenbräuker, "Characterization of vehicle-to-vehicle radio channels from measurements at 5.2 GHz," *Wireless Personal Commun.*, vol. 50, pp. 19–29, 2009.
- [17] J. Kunisch and J. Pamp, "Wideband car-to-car radio channel measurements and model at 5.9 GHz," in *Proc. IEEE Veh. Technol. Conf.*, 2008, DOI: 10.1109/VETEFC.2008.64.

- [18] L. Cheng, B. Henty, D. Stancil, F. Bai, and P. Mudalige, "Mobile vehicle-to-vehicle narrow-band channel measurement and characterization of the 5.9 GHz dedicated short range communication (DSRC) frequency band," *IEEE J. Sel. Areas Commun.*, vol. 25, no. 8, pp. 1501–1516, Oct. 2007.
- [19] G. Acosta-Marum and M. A. Ingram, "Six time- and frequency-selective empirical channel models for vehicular wireless LANs," *IEEE Veh. Technol. Mag.*, vol. 2, no. 4, pp. 4–11, Dec. 2007.
- [20] A. Paier, R. Tresch, A. Alonso, D. Smely, P. Meckel, Y. Zhou, and N. Czink, "Average downstream performance of measured IEEE 802.11p infrastructure-to-vehicle links," in *Proc. IEEE Int. Conf. Commun.*, Cape Town, South Africa, May 23–27, 2010, DOI: 10.1109/ICCW.2010.5503934.
- [21] A. F. Molisch, *Wireless Communications*, 2nd ed. New York: IEEE Press/Wiley, Nov. 2010.
- [22] L. Bernadó, T. Zemen, J. Karedal, A. Paier, A. Thiel, O. Klemp, N. Czink, F. Tufvesson, A. Molisch, and C. F. Mecklenbräuker, "Multi-dimensional k-factor analysis for V2V radio channels in open sub-urban street crossings," in *Proc. 21st Annu. IEEE Int. Symp. Personal Indoor Mobile Radio Commun.*, Istanbul, Turkey, Sep. 26–29, 2010, pp. 58–63.
- [23] J. Karedal, N. Czink, A. Paier, F. Tufvesson, and A. F. Molisch, "Pathloss modeling for vehicle-to-vehicle communications," *IEEE Trans. Veh. Technol.*, 2010, DOI: 10.1109/TVT.2010.2094632.
- [24] L. Bernadó, T. Zemen, A. Paier, G. Matz, J. Karedal, N. Czink, C. Dumard, F. Tufvesson, M. Hagenauer, A. F. Molisch, and C. F. Mecklenbräuker, "Non-WSSUS vehicular channel characterization at 5.2 GHz—Spectral divergence and time-variant coherence parameters," in *Proc. 29th URSI General Assembly*, Chicago, IL, Aug. 7–16, 2008, p. 198.
- [25] A. Paier, L. Bernadó, J. Karedal, O. Klemp, and A. Kwoczek, "Overview of vehicle-to-vehicle radio channel measurements for collision avoidance applications," in *Proc. IEEE Veh. Technol. Conf.*, 2010, DOI: 10.1109/VETECS.2010.5493975.
- [26] J. Karedal, F. Tufvesson, T. Abbas, O. Klemp, A. Paier, L. Bernadó, and A. F. Molisch, "Radio channel measurements at street intersections for vehicle-to-vehicle safety applications," in *Proc. IEEE Veh. Technol. Conf.*, 2010, DOI: 10.1109/VETECS.2010.5493955.
- [27] L. Reichardt, T. Fügen, and T. Zwick, "Influence of antennas placement on car to car communications channel," in *Proc. Eur. Conf. Antennas Propag.*, 2009, pp. 630–634.
- [28] O. Klemp, A. Thiel, A. Paier, L. Bernadó, J. Karedal, and A. Kwoczek, "In-situ vehicular antenna integration and design aspects for vehicle-to-vehicle communications," in *Proc. 9th COST2100 Management Committee Meeting*, Vienna, Austria, Sep. 2009, p. TD(09)982.
- [29] O. Klemp, "Performance considerations for automotive antenna equipment in vehicle-to-vehicle communications," in *Proc. URSI Int. Symp. Electromagn. Theory*, Berlin, Germany, Aug. 16–19, 2010, pp. 934–937.
- [30] L. Reichardt, T. Fügen, and T. Zwick, "Influence of antennas placement on car to car communications channel," in *Proc. Eur. Conf. Antennas Propag.*, 23–27, 2009, pp. 630–634.
- [31] *SIM-TDSichere Intelligente Mobilität—Testfeld Deutschland*. [Online]. Available: <http://www.simtd.de>
- [32] PRE-DRIVE C2X, *PREparation for DRIVING Implementation and Evaluation of C2X Communication Technology*. [Online]. Available: <http://www.pre-drive-c2x.eu>
- [33] V. Gonzalez-Posadas, D. Segovia-Vargas, E. Rajo-Iglesias, J. L. Vazquez-Roy, and C. Martin-Pascual, "Approximate analysis of short circuited ring patch antenna working at TM₀₁ mode," *IEEE Trans. Antennas Propag.*, vol. 54, no. 6, pp. 1875–1879, Jun. 2006.
- [34] A. Thiel and O. Klemp, "Initial results of multielement antenna performance in 5.85 GHz vehicle-to-vehicle scenarios," in *Proc. Eur. Microw. Conf.*, 27–31, 2008, pp. 1743–1746.
- [35] L. Reichardt, C. Sturm, and T. Zwick, "Performance evaluation of SISO, SIMO and MIMO antenna systems for car-to-car communications in urban environments," in *Proc. Int. Conf. Intell. Transport Syst. Telecommun.*, Oct. 20–22, 2009, pp. 51–56.
- [36] D. Kornek, M. Schack, E. Slotke, O. Klemp, I. Rolfes, and T. Kürner, "Effects of antenna characteristics and placements on a vehicle-to-vehicle channel scenario," in *Proc. IEEE Int. Conf. Commun.*, Cape Town, South Africa, May 23–27, 2010, DOI: 10.1109/ICCW.2010.5503935.
- [37] A. F. Molisch and F. Tufvesson, "Multipath propagation models for broadband wireless systems," in *Handbook of Signal Processing for Wireless Communications*, M. Ibnkahla, Ed. Boca Raton, FL: CRC Press, 2004.
- [38] A. F. Molisch, L. J. Greenstein, and M. Shafi, "Propagation issues for cognitive radio," *Proc. IEEE*, vol. 97, no. 5, pp. 787–804, May 2009.
- [39] M. Steinbauer and A. F. Molisch, *Directional Channel Modelling*. New York: Wiley, 2001, pp. 148–194.
- [40] A. F. Molisch, H. Asplund, R. Heddergott, M. Steinbauer, and T. Zwick, "The COST259 directional channel model—Part I: Overview and methodology," *IEEE Trans. Wireless Commun.*, vol. 5, no. 12, pp. 3421–3433, Dec. 2006.
- [41] H. Asplund, A. Glazunov, A. Molisch, K. Pedersen, and M. Steinbauer, "The COST 259 directional channel model—Part II: Macrocells," *IEEE Trans. Wireless Commun.*, vol. 5, no. 12, pp. 3434–3450, Dec. 2006.
- [42] A. F. Molisch and H. Hofstetter, "The COST 273 channel model," in *Mobile Broadband Multimedia Networks*. New York: Academic, 2006.
- [43] N. Costa and S. Haykin, *Multiple-Input, Multiple-Output Channel Models*. New York: Wiley, 2010, ser. Wiley Series in Adaptive and Learning Systems for Signal Processing, Communications, and Control.
- [44] C. Oestges, "Radio channel modeling for 4G networks," in *Pervasive Mobile & Ambient Wireless Communications*, 2011, ch. 3, in preparation.
- [45] G. Calcev, D. Chizhik, B. Goransson, S. Howard, H. Huang, A. Kogiantis, A. F. Molisch, A. L. Moustakas, D. Reed, and H. Xu, "A wideband spatial channel model for system-wide simulations," *IEEE Trans. Veh. Technol.*, vol. 56, no. 2, pp. 389–403, Mar. 2007.
- [46] P. Kyösti, J. Meinilä, L. Hentilä, X. Zhao, T. Jämsä, C. Schneider, M. Narandzić, M. Milojević, A. Hong, J. Ylitalo, V.-M. Holappa, M. Alatossava, R. Bultitude, Y. de Jong, and T. Rautiainen, "WINNER II Channel Models ver. 1.1," WINNER II Project, Tech. Rep. D1.1.2, Feb. 4, 2008.
- [47] W. Kim, H. Lee, J. J. Park, M.-D. Kim, and H. K. Chung, "Carrier frequency effects on propagation characteristics in rural macro environments," in *Proc. 4th Int. Conf. Commun. Netw. China*, 2009, DOI: 10.1109/CHINACOM.2009.5339780.
- [48] M. Failli, Ed., *Digital Land Mobile Radio Communications—COST 207*, ECSC-EEC-EAEC, 1989.
- [49] P. Driessen, "Prediction of multipath delay profiles in mountainous terrain," *IEEE J. Sel. Areas Commun.*, vol. 18, no. 3, pp. 336–346, Mar. 2000.
- [50] W. Mohr, "Wideband propagation measurements of mobile radio channels in mountainous areas in the 1800 MHz frequency range," in *Proc. IEEE Veh. Technol. Conf.*, 1993, pp. 49–52.
- [51] P. Pajusco, "Experimental characterization of doa at the base station in rural and urban area," in *Proc. IEEE Veh. Technol. Conf.*, 1998, vol. 2, pp. 993–997.
- [52] A. Algans, K. I. Pedersen, and P. E. Mogensen, "Experimental analysis of the joint statistical properties of azimuth spread, delay spread, and shadow fading," *IEEE J. Sel. Areas Commun.*, vol. 20, no. 3, pp. 523–531, Apr. 2002.
- [53] R. H. Clarke, "A statistical theory of mobile-radio reception," *Bell Syst. Tech. J.*, vol. 47, pp. 957–1000, Jul.–Aug. 1968.
- [54] W. C. Jakes, Ed., *Microwave Mobile Communications*. New York: Wiley, 1974.
- [55] M. Toeltsch, J. Laurila, K. Kalliola, A. F. Molisch, P. Vainikainen, and E. Bonek, "Statistical characterization of urban spatial radio channels," *IEEE J. Sel. Areas Commun.*, vol. 20, no. 3, pp. 539–549, Apr. 2002.
- [56] X. Zhao, J. Kivinen, P. Vainikainen, and K. Skog, "Propagation characteristics for wideband outdoor mobile communications at 5.3 GHz," *IEEE J. Sel. Areas Commun.*, vol. 20, no. 3, pp. 507–514, Apr. 2002.
- [57] E. S. Sousa, V. M. Jovanovic, and C. Daigneault, "Delay spread measurements for the digital cellular channel in Toronto," *IEEE Trans. Veh. Technol.*, vol. 43, no. 4, pp. 837–847, Nov. 1994.
- [58] T. S. Rappaport, S. Y. Seidel, and R. Singh, "900-MHz multipath propagation measurements for US digital cellular radiotelephone," *IEEE Trans. Veh. Technol.*, vol. 39, no. 2, pp. 132–139, May 1990.
- [59] A. Kuchar, J. P. Rossi, and E. Bonek, "Directional macro-cell channel characterization from urban measurements," *IEEE Trans. Antennas Propag.*, vol. 48, no. 2, pp. 137–146, Feb. 2000.
- [60] U. Martin, "Spatio-temporal radio channel characteristics in urban macrocells," *Inst. Electr. Eng. Proc.—Radar Sonar Navigat.*, vol. 145, pp. 42–49, Feb. 1998.
- [61] K. Kalliola, K. Sulonen, H. Laitinen, O. Kivekas, J. Krogerus, and P. Vainikainen, "Angular power distribution and mean effective gain of mobile antenna in different propagation environments," *IEEE Trans. Veh. Technol.*, vol. 51, no. 5, pp. 823–838, Sep. 2002.
- [62] X. Zhao, T. Rautiainen, K. Kalliola, and P. Vainikainen, "Path-loss models for urban microcells at 5.3 GHz," *IEEE Antennas*

- Wireless Propag. Lett.*, vol. 5, no. 1, pp. 152–154, Dec. 2006.
- [63] L. Vuokko, V.-M. Kolmonen, J. Salo, and P. Vainikainen, “Measurement of large-scale cluster power characteristics for geometric channel models,” *IEEE Trans. Antennas Propag.*, vol. 55, no. 11, pp. 3361–3365, Nov. 2007.
- [64] M. J. Feuerstein, K. L. Blackard, T. S. Rappaport, S. Y. Seidel, and H. H. Xia, “Path loss, delay spread, and outage models as functions of antenna height for microcellular system design,” *IEEE Trans. Veh. Technol.*, vol. 43, no. 3, pp. 487–498, Aug. 1994.
- [65] S. Kozono and A. Taguchi, “Mobile propagation loss and delay spread characteristics with a low base station antenna on an urban road,” *IEEE Trans. Veh. Technol.*, vol. 42, no. 1, pp. 103–109, Feb. 1993.
- [66] G. Ching, M. Ghorashi, M. Landmann, N. Lertsirisopon, J. Takada, T. Imai, I. Samedá, and H. Sakamoto, “Wideband polarimetric directional propagation channel analysis inside an arched tunnel,” *IEEE Trans. Antennas Propag.*, vol. 57, no. 3, pp. 760–767, Mar. 2009.
- [67] M. Lienard and P. Degauque, “Natural wave propagation in mine environments,” *IEEE Trans. Antennas Propag.*, vol. 48, no. 9, pp. 1326–1339, Sep. 2000.
- [68] Y. P. Zhang and Y. Hwang, “Characterization of UHF radio propagation channels in tunnel environments for microcellular and personal communications,” *IEEE Trans. Veh. Technol.*, vol. 47, no. 1, pp. 283–296, Feb. 1998.
- [69] A. Paier, J. Karedal, N. Czink, H. Hofstetter, C. Dumard, T. Zemen, F. Tufvesson, C. F. Mecklenbräuer, and A. F. Molisch, “First results from car-to-car and car-to-infrastructure radio channel measurements at 5.2 GHz,” in *Proc. IEEE Int. Symp. Personal Indoor Mobile Radio Commun.*, 2007, DOI: 10.1109/PIMRC.2007.4394143.
- [70] J. Maurer, T. Fügen, and W. Wiesbeck, “Narrow-band measurement and analysis of the inter-vehicle transmission channel at 5.2 GHz,” in *Proc. IEEE Veh. Technol. Conf.*, 2002, pp. 1274–1278.
- [71] P. Paschalidis, M. Wisotzki, A. Kortke, W. Keusgen, and M. Peter, “A wideband channel sounder for car-to-car radio channel measurements at 5.7 GHz and results for an urban scenario,” in *Proc. IEEE Veh. Technol. Conf.*, Sep. 2008, DOI: 10.1109/VETECF.2008.62.
- [72] I. Tan, W. Tang, K. Laberteaux, and A. Bahai, “Measurement and analysis of wireless channel impairments in DSRC vehicular communications,” in *Proc. IEEE Int. Conf. Commun.*, 2008, pp. 4882–4888.
- [73] A. Paier, J. Karedal, N. Czink, H. Hofstetter, C. Dumard, T. Zemen, F. Tufvesson, A. F. Molisch, and C. F. Mecklenbräuer, “Car-to-car radio channel measurements at 5 GHz: Pathloss, power-delay profile, and delay-Doppler spectrum,” in *Proc. Int. Symp. Wireless Commun. Syst.*, 2007, pp. 224–228.
- [74] L. Cheng, B. E. Henty, F. Bai, and D. D. Stancil, “Highway and rural propagation channel modeling for vehicle-to-vehicle communications at 5.9 GHz,” in *Proc. IEEE Antennas Propag. Soc. Int. Symp.*, 2008, DOI: 10.1109/APS.2008.4619037.
- [75] J. Mittag, S. Papanatiassiou, H. Hartenstein, and E. Ström, “Enabling accurate cross-layer PHY/MAC/NET simulation studies of vehicular communication networks,” *Proc. IEEE Special Issue on Vehicular Communications*, Jun. 2011.
- [76] *IEEE P802.11p/D0.26: Part 11: Wireless LAN Medium Access Control (MAC) and Physical Layer (PHY) Specifications: Amendment 3: Wireless Access in Vehicular Environments (WAVE)*, Draft 0.26, Jan. 2006.
- [77] J. Maurer, T. Fügen, T. Schafer, and W. Wiesbeck, “A new inter-vehicle communications (IVC) channel model,” in *Proc. IEEE Veh. Technol. Conf.*, 2004, pp. 9–13.
- [78] W. Wiesbeck and S. Knorz, “Characteristics of the mobile channel for high velocities,” in *Proc. Int. Conf. Electromagn. Adv. Appl.*, 2007, pp. 116–120.
- [79] L. C. Wang, W. C. Liu, and Y. H. Cheng, “Statistical analysis of a mobile-to-mobile Rician fading channel model,” *IEEE Trans. Veh. Technol.*, vol. 58, no. 1, pp. 32–38, Jan. 2009.
- [80] A. Zajic and G. Stuber, “Three-dimensional modeling and simulation of wideband MIMO mobile-to-mobile channels,” *IEEE Trans. Wireless Commun.*, vol. 8, no. 3, pp. 1260–1275, Mar. 2009.
- [81] X. Cheng, C.-X. Wang, D. I. Laurenson, S. Salous, and A. V. Vasiliakos, “An adaptive geometry-based stochastic model for non-isotropic mimo mobile-to-mobile channels,” *IEEE Trans. Wireless Commun.*, vol. 8, no. 9, pp. 4824–4835, Sep. 2009.
- [82] M. Pätzold, B. Hogstad, and N. Youssef, “Modeling, analysis, and simulation of MIMO mobile-to-mobile fading channels,” *IEEE Trans. Wireless Commun.*, vol. 7, no. 2, pp. 510–520, Feb. 2008.
- [83] T. M. Wu and C. Kuo, “3-D space-time-frequency correlation functions of mobile-to-mobile radio channels,” in *Proc. IEEE Veh. Technol. Conf.*, 2007, pp. 334–338.
- [84] A. Zajic and G. Stuber, “Statistical properties of wideband MIMO mobile-to-mobile channels,” in *Proc. IEEE Wireless Commun. Netw. Conf.*, 2008, pp. 763–768.
- [85] J. Karedal, F. Tufvesson, N. Czink, A. Paier, C. Dumard, T. Zemen, C. F. Mecklenbräuer, and A. F. Molisch, “A geometry-based stochastic MIMO model for vehicle-to-vehicle communications,” *IEEE Trans. Wireless Commun.*, vol. 8, no. 7, pp. 3646–3657, Jul. 2009.
- [86] N. Czink, F. Kaltenberger, Y. Zhou, L. Bernadó, T. Zemen, and X. Yin, “Low-complexity geometry-based modeling of diffuse scattering,” in *Proc. Eur. Conf. Antennas Propag.*, Barcelona, Spain, Apr. 12–16, 2010.
- [87] *Wireless LAN Medium Access Control (MAC) and Physical Layer (PHY) Specifications*, IEEE Standard 802.11-2007: Part 11, Jun. 12, 2007.
- [88] Z. Wang and G. B. Giannakis, “Wireless multicarrier communications,” *IEEE Signal Process. Mag.*, vol. 17, no. 3, pp. 29–48, May 2000.
- [89] S. B. Weinstein and P. M. Ebert, “Data transmission by frequency-division multiplexing using the discrete Fourier transform,” *IEEE Trans. Commun.*, vol. 19, no. 5, pp. 628–634, Oct. 1971.
- [90] G. Faria, J. A. Henriksson, E. Stare, and P. Talmola, “DVB-H: Digital broadcast services to handheld devices,” *Proc. IEEE*, vol. 94, no. 1, pp. 194–209, Jan. 2006.
- [91] H. Sari, G. Karam, and I. Jeanclaude, “Transmission techniques for digital terrestrial time-variant broadcasting,” *IEEE Commun. Mag.*, vol. 33, no. 2, pp. 100–109, Feb. 1995.
- [92] ETSI, *Digital Video Broadcasting (DVB): Framing Structure, Channel Coding and Modulation for Digital Terrestrial Television*, ETSI EN 300 744 V1.4.1, Jan. 2001. [Online]. Available: <http://www.etsi.org>
- [93] ETSI, *Digital Audio Broadcasting (DAB) to Mobile, Portable and Fixed Receivers*, ETSI EN 300 401, May 2001. [Online]. Available: <http://www.etsi.org>
- [94] ETSI, *Digital Radio Mondiale (DRM): System Specification*, ETSI ES 201 980 V2.1.1, Apr. 2004. [Online]. Available: <http://www.etsi.org>
- [95] E. Dahlman, S. Parkvall, J. Skold, and P. Beming, *3G Evolution: HSPA and LTE for Mobile Broadband*. New York: Academic, 2008.
- [96] B. O’Hara and A. Petrick, *The IEEE 802.11 Handbook: A Designer’s Companion*. Piscataway, NJ: IEEE Press, 2005.
- [97] L. Bernadó, T. Zemen, N. Czink, and P. Belanovic, “Physical layer simulation results for IEEE 802.11p using vehicular non-stationary channel model,” in *Proc. IEEE Int. Conf. Commun.*, Cape Town, South Africa, May 23–27, 2010, DOI: 10.1109/ICCW.2010.5503942.
- [98] J. van de Beek, O. Edfors, M. Sandell, S. Wilson, and P. Borjesson, “On channel estimation in OFDM systems,” in *Proc. IEEE Veh. Technol. Conf.*, Jul. 1995, vol. 2, pp. 815–819.
- [99] Y. Shen and E. Martinez, “Channel estimation in OFDM systems,” Freescale Semiconductor, Inc., Applicat. Note AN3059, Jan. 2006.
- [100] S. Coleri, M. Ergen, A. Puri, and A. Bahai, “Channel estimation techniques based on pilot arrangement in OFDM systems,” *IEEE Trans. Broadcast.*, vol. 48, no. 3, pp. 223–229, Sep. 2002.
- [101] CohdaWireless, “Mobility and multipath: Challenges for DSRC,” whitepaper, Sep. 2009.
- [102] A. Doukas and G. Kalivas, “Performance analysis of a channel estimator using linear interpolation for OFDM systems,” in *Proc. 40th Asilomar Conf. Signals Syst. Comput.*, Nov. 1–29, 2006, pp. 1786–1790.
- [103] J. Park, J. Kim, C. Kang, and D. Hong, “Channel estimation performance analysis for comb-type pilot-aided OFDM systems with residual timing offset,” in *Proc. IEEE Veh. Technol. Conf.*, Sep. 2004, vol. 6, pp. 4376–4379.
- [104] S. Kaul, K. Ramachandran, P. Shankar, S. Oh, M. Gruteser, I. Seskar, and T. Nadeem, “Effect of antenna placement and diversity on vehicular network communications,” in *Proc. 4th Annu. IEEE Commun. Soc. Conf. Sensor Mesh Ad Hoc Commun. Netw.*, 18–21, 2007, pp. 112–121.
- [105] S. Fikar, W. Walzik, and A. L. Scholtz, “Vehicular multi/broadband MIMO antenna for terrestrial communication,” in *Proc. IEEE Antennas Propag. Soc. Int. Symp.*, Toronto, ON, Canada, Jul. 2010, DOI: 10.1109/APS.2010.5561239.
- [106] C. Squires and T. Willink, “The impact of vehicular antenna placement on polarization diversity,” in *Proc. IEEE Veh. Technol. Conf.*, 20–23, 2009, DOI: 10.1109/VETECF.2009.5379017.
- [107] M. Wellens, B. Westphal, and P. Mahonen, “Performance evaluation of IEEE

- 802.11-based WLANs in vehicular scenarios," in *Proc. IEEE Veh. Technol. Conf.*, Apr. 2007, pp. 1167–1171.
- [108] L. Cheng, B. E. Henty, R. Cooper, and D. D. Stancil, "A measurement study of time-scaled 802.11a waveforms over the mobile-to-mobile vehicular channel at 5.9 GHz," *IEEE Commun. Mag.*, vol. 46, no. 5, pp. 84–91, May 2008.
- [109] D. Jiang and L. Delgrossi, "IEEE 802.11p: Towards an international standard for wireless access in vehicular environments," in *Proc. IEEE Veh. Technol. Conf.*, May 2008, pp. 2036–2040.
- [110] S. Eichler, "Performance evaluation of the IEEE 802.11p WAVE communication standard," in *Proc. IEEE Veh. Technol. Conf.*, Sep. 2007, pp. 2199–2203.
- [111] L. Stibor, Y. Zang, and H.-J. Reuerman, "Evaluation of communication distance of broadcast messages in a vehicular ad-hoc network using IEEE 802.11p," in *Proc. IEEE Wireless Commun. Netw. Conf.*, Mar. 2007, pp. 254–257.
- [112] J. Eriksson, H. Balakrishnan, and S. Madden, "Cabernet: Vehicular content delivery using WiFi," in *Proc. 14th ACM MOBICOM*, San Francisco, CA, Sep. 2008, pp. 199–210.
- [113] P. Lutterotti, G. Pau, D. Jiang, M. Gerla, and L. Delgrossi, "C-VeT, the UCLA vehicular testbed: An open platform for vehicular networking and urban sensing," in *Proc. Int. Conf. Wireless Access Veh. Environ.*, Dearborn, MI, Dec. 2008, pp. 1–9.
- [114] CVIS, *Cooperative Vehicle—Infrastructure Systems*. [Online]. Available: <http://www.cvisproject.org>
- [115] K. Sjöberg-Bilstrup, E. Uhlemann, and E. G. Ström, "Scalability issues of the MAC methods STDMA and CSMA of IEEE 802.11p when used in VANETs," in *Proc. IEEE Int. Conf. Commun.*, Cape Town, South Africa, May 23–27, 2010, DOI: 10.1109/ICCW.2010.5503941.

ABOUT THE AUTHORS

Christoph F. Mecklenbräuker (Senior Member, IEEE) received the Dipl.-Ing. degree in electrical engineering from the Technische Universität Wien, Vienna, Austria, in 1992 and the Dr.-Ing. degree from the Ruhr-Universität Bochum, Bochum, Germany, in 1998, both with distinction. His doctoral dissertation on matched field processing received the Gert-Massenberg Prize in 1998.

He was with Siemens, Vienna, Austria, from 1997 to 2000. He was a delegate to the Third Generation Partnership Project (3GPP) and engaged in the standardization of the radio access network for the Universal Mobile Telecommunications System (UMTS). From 2000 to 2006, he has held a senior research position with the Telecommunications Research Center Vienna (FTW), Vienna, Austria, in the field of mobile communications. In 2006, he joined the Faculty of Electrical Engineering and Information Technology as a Full Professor with the Technische Universität Wien. Since 2009, he has been leading the Christian Doppler Laboratory for Wireless Technologies for Sustainable Mobility. He has authored approximately 100 papers in international journals and conferences, for which he has also served as a reviewer, and holds eight patents in the field of mobile cellular networks. His current research interests include vehicular connectivity, ultrawideband (UWB) radio, and multiple-input-multiple-output (MIMO) techniques for wireless systems.

Dr. Mecklenbräuker is a member of the IEEE Signal Processing, Antennas and Propagation, and Vehicular Technology Societies, as well as Verband der Elektrotechnik Elektronik Informationstechnik e.V. and the European Association for Signal Processing (EURASIP).

Andreas F. Molisch (Fellow, IEEE) received his Dipl. Ing., (M.Sc.), Ph.D. and habilitation degrees in Electrical Engineering in 1990, 1994, and 1999, respectively, all from Technische Universität Wien, Vienna, Austria.

He is currently Professor of Electrical Engineering at the University of Southern California, Los Angeles. Previously, he was with AT&T (Bell) Laboratories Research (USA), Lund University (Sweden), Mitsubishi Electric Research Labs, (USA), and Technical University of Vienna (Austria). His current research interests are measurement and modeling of mobile radio channels, ultrawideband (UWB), cooperative communications, and multiple-input-multiple-output (MIMO) systems. He has authored, coauthored, or edited four books [among them the textbook *Wireless Communications* (New York: Wiley/IEEE Press, 2005)], 11 book chapters, more than 120 journal papers, and numerous conference contributions, as well as more than 70 patents and 60 standards contributions.

Dr. Molisch has been an editor of a number of journals and special issues, General Chair, TPC Chair, or Symposium Chair of multiple international conferences, and chairman of various international standardization groups. He is a Fellow of the Institution of Engineering and Technology (IET), an IEEE Distinguished Lecturer, and recipient of several awards.



Johan Karedal (Member, IEEE) received the M.S. degree in engineering physics and the Ph.D. degree in electrical engineering from Lund University, Lund, Sweden, in 2002 and 2009, respectively.

Currently, he is an Assistant Professor at the Department of Electrical and Information Technology, Lund University, where his main research interests concern measurements and modeling of wireless propagation channels.



Fredrik Tufvesson (Senior Member, IEEE) was born in Lund, Sweden, in 1970. He received the M.S. degree in electrical engineering, the Licentiate degree, and the Ph.D. degree in electrical engineering from Lund University, Lund, Sweden, in 1994, 1998, and 2000, respectively.

After almost two years at a startup company, Fiberless Society, he is now an Associate Professor at the Department of Electrical and Information Technology, Lund University. His main research interests are channel measurements and modeling for wireless communication, including channels for both multiple-input-multiple-output (MIMO) and ultrawideband (UWB) systems. In addition, he also works with his company ResQU on wireless search and rescue equipment as well as research projects on OFDM and UWB system design.



Alexander Paier (Student Member, IEEE) was born in Bruck/Mur, Austria. He received the Dipl.-Ing. (M.Sc.) and Ph.D. degrees (with distinction) in electrical engineering from Vienna University of Technology, Vienna, Austria, in 2006 and 2009, respectively.

Since 2006, he has been affiliated with the Institute of Communications and Radio-Frequency Engineering, Vienna University of Technology. He actively contributed to the Special Interest Group "Mobile to Mobile Communications" within COST Action 2100 "Pervasive Mobile and Ambient Wireless Communications." He was responsible for several measurement campaigns for vehicular communications. His current research interests include vehicular multiple-input-multiple-output (MIMO) channel measurements and characterization for safety-related vehicular networks.



Mecklenbräuker *et al.*: Vehicular Channel Characterization and Its Implications

Laura Bernadó (Student Member, IEEE) received the M.Sc. degree in telecommunications engineering from the Technical University of Catalonia (UPC), Barcelona, Spain, in 2007, with her thesis written at the Radio Communications Department of the Royal Institute of Technology (KTH), Stockholm, Sweden. Currently, she is working towards the Ph.D. degree at the Vienna University of Technology, Vienna, Austria.



Since January 2008, she has been with the Telecommunications Research Center Vienna (FTW), Vienna, Austria, working as a Researcher in safety-related vehicular communications projects. Her research interests are modeling of fast time-varying fading processes, and particularly characterization of nonstationarity for vehicular channels.

Thomas Zemen (Senior Member, IEEE) was born in Mödling, Austria. He received the Dipl.-Ing. degree (with distinction) in electrical engineering from Vienna University of Technology, Vienna, Austria, in 1998 and the Ph.D. degree in electrical engineering (with distinction) in 2004.



He joined Siemens Austria in 1998 where he worked as a Hardware Engineer and Project Manager for the Radio Communication Devices Department. Since October 2003, he has been with the Telecommunications Research Center Vienna (FTW), Vienna, Austria. His research interests include cooperative communication systems, software-defined radio concepts, vehicle-to-vehicle channel measurements and modeling, orthogonal frequency division multiplexing (OFDM), multiuser detection, time-variant channel estimation, iterative multiple-input-multiple-output (MIMO) receiver structures, cooperative localization, interference management, and energy-neutral sensor networks. Since 2008, he has been the Department Head for “Signal and Information Processing” at FTW. He is the speaker of the national research network for “Signal and Information Processing in Science and Engineering” funded by the Austrian Science Fund (FWF). He teaches “cooperative communications” as external lecturer at Vienna University of Technology.

Oliver Klemp (Member, IEEE) was born in Hannover, Germany, in 1976. He received the Dipl.-Ing. degree and the Dr.-Ing. degree (with distinction) in electrical engineering from Leibniz University of Hannover, Hannover, Germany, in 2002 and 2007, respectively.



His principal research interests include multi-antenna systems, channels and electronics for wireless multiple-input-multiple-output (MIMO), and ultrawideband (UWB) communications. He joined Delphi Delco Electronics Europe in 2006 as a Research Engineer for antennas and receivers in the area of digital satellite radio systems. From 2007 through 2010, he worked as a Product Line Architect and Project Manager in advanced engineering and series development with focus on antennas and transceivers for vehicle-to-vehicle communications and automotive infotainment systems. In 2010, he joined BMW Group Research and Development, Munich, Germany, as a Research Specialist in the area of vehicle-centric communications. Since 2007, he has been also teaching “RF transmit & receive circuits” and “electromagnetic wave propagation” as an external lecturer at Leibniz University of Hannover. He has authored or coauthored more than 50 papers in international journals and conferences and also serves as a reviewer.

Dr. Klemp was awarded the “Gerotron Innovation Award” in 2005 and is the recipient of the “Science Award of the City of Hannover 2008.” He is a member of the German Electrotechnical Association (VDE), COST 2100, and the Car-2-Car Communication Consortium.

Nicolai Czink (Member, IEEE) received the Dipl.-Ing. (M.S.) and the Dr.techn. (Ph.D.) degrees in electrical engineering from Vienna University of Technology, Vienna, Austria, with distinction, in 2004 and 2007, respectively. His Ph.D. dissertation received an award from the Austrian Electrotechnical Association (OVE).



After his Ph.D., he joined Stanford University, Stanford, CA, as a Postdoctoral Researcher on an Erwin Schrödinger Fellowship of the FWF Austrian Science Fund. He is currently Senior Researcher at the FTW Telecommunications Research Center Vienna, Vienna, Austria, being an expert in channel modeling, cooperative communications, and intelligent transportation systems. He is the author of more than 50 research papers and communications in international journals and conferences.